Science of the Total Environment 838 (2022) 156542

Contents lists available at ScienceDirect

Science of the Total Environment

journal homepage: www.elsevier.com/locate/scitotenv

The glacial–terrestrial–fluvial pathway: A multiparametrical analysis of spatiotemporal dissolved organic matter variation in three catchments of Lake Nam Co, Tibetan Plateau

Philipp Maurischat [a,*], Lukas Lehnert [b], Vinzenz H.D. Zerres [b], Tuong Vi Tran [c], Karsten Kalbitz [d], Åsmund Rinnan [e], Xiao Gang Li [f], Tsechoe Dorji [g], Georg Guggenberger [a]

[a] Leibniz University Hannover, Institute of Soil Science, Hannover, Germany
[b] Ludwig-Maximilians-Universität München, Department of Geography, Munich, Germany
[c] Leibniz University Hannover, Institute of Fluid Mechanics and Environmental Physics in Civil Engineering, Hannover, Germany
[d] Technische Universität Dresden, Institute of Soil Science and Site Ecology, Dresden, Germany
[e] University of Copenhagen, Department of Food Science, Copenhagen, Denmark
[f] School of Life Sciences, Lanzhou University, Lanzhou, China
[g] Key Laboratory of Alpine Ecology and Biodiversity, Institute of Tibetan Plateau Research, Chinese Academy of Sciences, Lhasa, Tibet Autonomous Region, China

HIGHLIGHTS

- First multiparametrical DOM study for several catchments of a large Tibetan lake
- Lake and stream water DOM are chemically distinct.
- Influence of catchment properties on stream DOM indicates different DOM sources.
- Terrestrial influence on stream DOM composition is greatest in low order streams.
- The Indian summer monsoon greatly modifies stream DOM composition in the catchments.

GRAPHICAL ABSTRACT

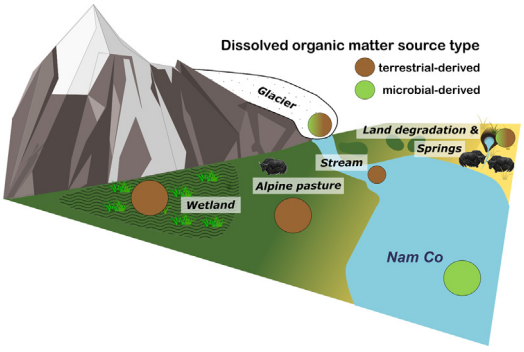

ARTICLE INFO

Editor: Daniel Alessi

Keywords:
Alpine pastures
Dissolved organic carbon
PARAFAC
Fluorescence
Tibetan plateau
Third pole environment

ABSTRACT

The Tibetan Plateau (TP) is a sensitive alpine environment of global importance, being Asia's water tower, featuring vast ice masses and comprising the world's largest alpine grasslands. Intensified land-use and pronounced global climate change have put pressure on the environment of the TP. We studied the tempo-spatial variability of dissolved organic matter (DOM) to better understand the fluxes of nutrients and energy from terrestrial to aquatic ecosystems in the TP. We used a multiparametrical approach, based on inorganic water chemistry, dissolved organic carbon (DOC) concentration, dissolved organic matter (DOM) characteristics (chromophoric DOM, fluorescence DOM and $\delta^{13}C$ of DOM) in stream samples of three catchments of the Nam Co watershed and the lake itself. Satellite based plant cover estimates were used to link biogeochemical data to the structure and degradation of vegetation zones in the catchments. Catchment streams showed site-specific DOM signatures inherited from glaciers, wetlands, groundwater, and *Kobresia pygmaea* pastures. By comparing stream and lake samples, we found DOM processing and unification by loss of chromophoric DOM signatures and a change towards an autochthonous source of lake DOM. DOM diversity was largest in the headwaters of the catchments and heavily modified in terminal aquatic systems. Seasonality was characterized by a minor influence of freshet and by a very strong impact of the Indian summer monsoon on DOM composition, with more microbial DOM sources. The DOM of Lake Nam Co differed chemically from stream water samples,

* Corresponding author.
E-mail address: maurischat@ifbk.uni-hannover.de (P. Maurischat).

http://dx.doi.org/10.1016/j.scitotenv.2022.156542
Received 22 February 2022; Received in revised form 2 June 2022; Accepted 3 June 2022
Available online 9 June 2022

indicating the lake to be a quasi-marine environment in regards to the degree of chemical modification and sources of DOM. DOM proved to be a powerful marker to elucidate consequences of land use and climatic change on biogeochemical processes in High Asian alpine ecosystems.

1. Introduction

Dissolved organic matter (DOM) is composed of various organic substances ≤ 0.45 μm and is an important nutrient and energy source in aquatic and terrestrial ecosystems (Wymore et al., 2016). DOM is part of the global carbon cycle (Roulet and Moore, 2006), and often the majority of ecosystem carbon losses occur via DOM export (Lau, 2021). The observed huge variability in the concentration of dissolved organic carbon (DOC) and DOM composition in surface waters reflects the characteristics of and processes within a respective catchment (Jaffé et al., 2012; Kawahigashi et al., 2004; Singer et al., 2012).

DOM bridges glacial, terrestrial, lotic (riverine) and limnic ecosystems, and shows pronounced effects of seasonality in composition and mobility. DOM is an indicator of environmental changes, triggered for example by acidification (Han et al., 2022a; Guggenberger, 1994), altered soil thermal regimes (Kawahigashi et al., 2004), or eutrophication (Görs et al., 2007). Changes in biodiversity can be driven by DOM (Zhao et al., 2019), when highly biodegradable compounds enter oligotrophic estuaries (Görs et al., 2007).

The process of DOM formation largely depends on the catchment area and therefore is also affected by the biogeodiversity of catchments (Coch et al., 2019; Lafrenière and Sharp, 2004), climatic processes (Song et al., 2020) and the impact of seasonality (Jennings et al., 2020). DOM diversity peaks in first order streams and then decreases with increasing stream order (Mosher et al., 2015). DOM is processed and chemically altered during its fluvial pathway in streams (Riedel et al., 2016) and lakes (Massicotte and Frenette, 2013), thereby changing its signature and ultimately forming terminal characteristics (Riedel et al., 2016). Universal processes of DOM degradation in rivers and estuaries, lead to successive loss of terrigenous DOM signatures and finally to molecular conformity of DOM (Zark and Dittmar, 2018).

The Tibetan Plateau (TP) is of global importance and affects multiple scales and processes. The TP comprises the largest ice mass outside of the Polar regions (Qiu, 2008; Yao et al., 2012) and is a glacial hotspot. High Asian watersheds play a decisive role for Asian lowlands and even for marine environments in South Asia (Xu et al., 2021). The TP features the largest alpine grassland of the world (Miehe et al., 2019), and large alpine wetlands (Zhang et al., 2020) with active pastoralism (Gongbuzeren and Li, 2018). Alpine wetlands remain the least studied terrestrial biome in the TP (Anslan et al., 2020), while degradation of wetlands is already underway (Zhang et al., 2020) with severe consequences that lead to the release of considerable amounts of chromophoric DOM.

Sensitive high-altitude ecosystems, especially the vast grasslands of the TP are under pressure by several threats such as intensified land-use and pronounced global warming (Harris, 2010). Gaining knowledge on biogeochemistry processes within the TP is an essential component for understanding current challenges. Still, implications on DOM formation, characteristics, and fate are seldom addressed in studies that deal with the effects of grassland degradation (Anslan et al., 2020) and disregard the evidence that DOM is a proven marker for terrestrial degradation processes (Coch et al., 2019; Jennings et al., 2020; Lafrenière and Sharp, 2004; Yamashita et al., 2010). As a marker, DOM can help to upscale plot based investigations to landscape level (Speetjens et al., 2020). Pasture degradation translates to several threats, for limnic systems, such as increased water temperatures (Gao, 2016) or adverse impacts on lake biodiversity (Kritzberg et al., 2020).

The rapid temperature increase of the TP (Song et al., 2020) has led to changes, foremost in glaciated catchments (Bolch et al., 2010). Glaciers possess unique DOM signatures (Boix Canadell et al., 2019; Hood et al., 2009) with accelerating climate-driven export of DOM into downstream water bodies. Still, there is only limited knowledge on how current glacier wastage influences DOM and impacts downstream catchments of High Asia. Spatiotemporal changes in DOM composition of terminal aquatic systems, such as endorheic lakes, can be utilised to monitor responses of biogeochemistry in ecosystems upstream. Endorheic basins provide an excellent opportunity to investigate ecosystem processes as they are influenced by environmental change. In our study, we focus on the oligotrophic (Hu et al., 2016), endorheic Lake Nam Co. Increases of the lake level of Nam Co were reported for the last decades (Wang et al., 2009), likely affecting the chemistry of the saline and alkaline lake (Wang et al., 2020). The chemical composition of the lake water is influenced by evaporation and crystallization, leading to an enrichment of most ions compared to streams and wetland sources (Wang et al., 2010).The lake receives stream DOM from its diverse watershed and also forms the terminus of a potential DOM degradation cascade. The physico-chemistry of stream water was reported to be connected to the local geology in the catchments, while being primarily influenced by total runoff (Yu et al., 2019), the latter likely increases under warmer conditions triggering glacial wastage. The Nam Co watershed is spatially very diverse, and comprises glaciers and periglacial landforms, alpine steppe, alpine wetlands and *Kobresia pygmaea* alpine pasture/meadow biomes in different degrees of plant cover and pasture degradation. Alpine pastures are predominantly developed in the mid and higher slopes as well as in depressions, and alpine steppe is mostly developed in the arid lake foreland. The streams of the watershed are fed by glacial melt, precipitation and groundwater (Adnan et al., 2019), depending on catchment properties, such as aspect and elevation. The Lake Nam Co watershed is a suited natural laboratory to study controlling factors of the spatiotemporal variability of DOM in this sensitive area.

This study aims to identify the impact of small-scale catchment properties, referred to as endmembers and season on the origin and composition of riverine DOM. We further aimed at elucidating the mechanisms that control DOM processing along the fluvial pathways to Lake Nam Co. We tested whether DOM characteristics are connected to landscape units and biomes in the catchments, with fundamental differences between alpine steppe, alpine pastures and alpine wetland riverine DOM. We particularly assumed that DOM composition is largely determined by catchment hydrology and the degree of green plant cover and that unique signatures of glacial meltwater, precipitation-fed and groundwater-fed areas can be discriminated. Furthermore, we assessed the impact of seasonality on DOM composition. We hypothesized that 1) catchment biogeodiversity in the Nam Co watershed governs DOM and water chemistry. During the fluvial pathway, chromophoric DOM and readily bioavailable compounds will be preferentially altered. Consequently, we further hypothesized that 2) the endorheic Lake Nam Co is the terminal point of a DOM degradation cascade showing transformed, and seasonally stable DOM signatures.

To understand the complex environmental implications between glacial, terrestrial, lotic and limnic ecosystem of the Nam Co watershed, we applied a DOM multiparameter approach to three catchments as well as the Lake Nam Co. To link DOM characteristics to the vegetation cover and its changes, we conducted a satellite-based watershed-wide estimation of plant cover in 30 m resolution for an observation period of 30 years (1990–2020).

2. Materials and methods

2.1. Study area

Lake Nam Co (4726 m asl.) covers >2000 km^2, with a total watershed area of 10,789 km^2 (Fig. 1). The Nyainqêntanglha mountain ridge with elevations up to 7000 m asl. forms the south and south-eastern border of the

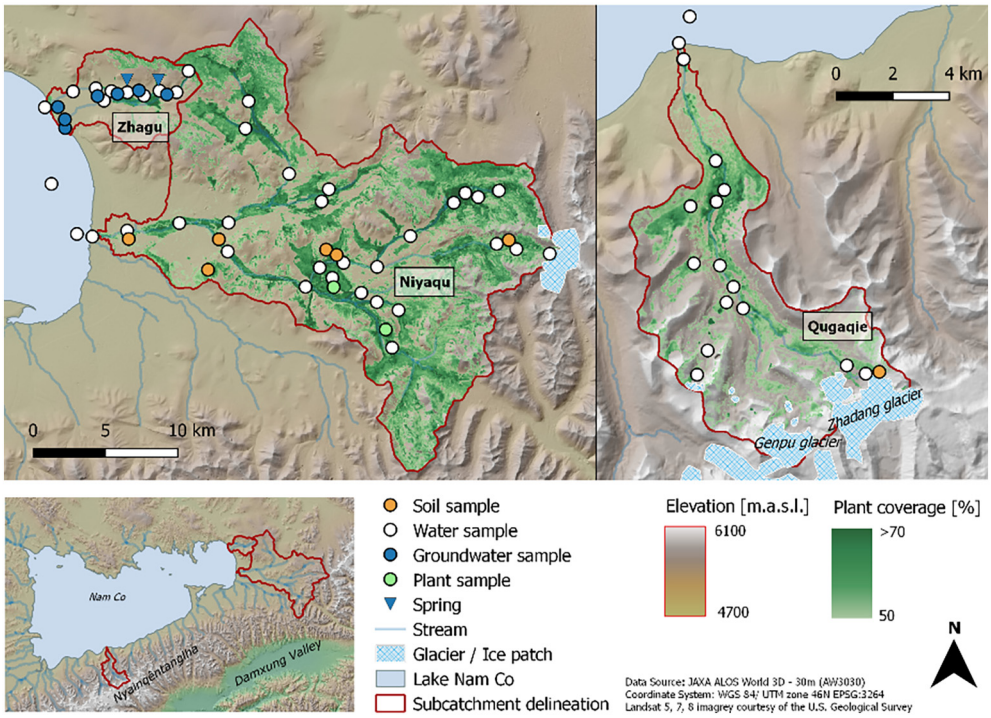

Fig. 1. Overview of the investigated catchments including positions of sampling sites.

watershed. It comprises a well-investigated glacial environment (Bolch et al., 2010; Buckel et al., 2020). The northern region of the watershed in contrary, is dominated by hilly uplands (Yu et al., 2021). Sparse alpine vegetation exists in the glacial foreland at elevations >5350 m asl., while *Kobresia pygmaea (K. pygmaea)* pastures dominate up to 4900 m asl. At lower elevations, an ecotone between *K. pygmaea* pastures and the alpine steppe biome is developed. The alpine steppe is fully developed in the lowlands close to the lake shore (Miehe et al., 2019). Alpine wetlands are found in depressions (Anslan et al., 2020), and often formed through riverine influence. Degradation and aridity are increasing along the south-north gradient of the watershed (Anslan et al., 2020).

The mean annual temperature at Lake Nam Co is 0.6 °C and the mean annual precipitation ranges from 405 mm at the southern lake shore to 300 mm at the watersheds northern margin (Anslan et al., 2020). Lake Nam Co's climate is biannual with cold and dry winters and minimal air temperature below −20 °C between December and February, with sparse precipitation events and typical absence of a closed snow cover (Dorji et al., 2013). The Indian summer monsoon (ISM) starts around May to June, whereby moist and warm air masses are shifted from the Indian subcontinent towards the inner TP. 80% of the annual precipitation falls during the ISM (until September), and the mean day-time air temperature reaches 11 °C (Chen et al., 2019). The ISM is the most influential hydrological and temperature control factor in our study area (Nieberding et al., 2021).

Within the Nam Co watershed, three catchments were selected to represent the differing abiotic and biotic environment in the watershed, such as: degree of plant cover, status of degradation, presence of groundwater springs and alpine wetlands, elevation and extent of glaciation. The study area includes the catchments of the streams Niyaqu, east of Lake Nam Co, Zhagu north-east of the lake, and Qugaqie, south-west of Lake Nam Co (Fig. 1). Our dataset consists of samples from three higher order (>3) rivers and 12 lower order streams (1–3) of these catchments and from the lake.

The Niyaqu catchment covers 406 km^2. A major river with two river arm systems drains the catchment. The southern stream comprises glacial zones and runs through an area of extended alpine pastures (Fig. 2a) and an alpine wetland (Fig. 2c). The northern river arm system is characterized by the absence of glacial meltwater and a hilly upland relief, situated in the pasture - steppe ecotone. The Niyaqu catchment is used for yak grazing throughout the year. Its valley course is mostly in west-east direction with a high altitudinal gradient between the lake shore and the eastern branch of Nyainqêntanglha (peaking at 5680 m asl. within Niyaqu catchment).

The Qugaqie catchment comprises an area of 58 km^2. It is situated at the flank of the Nyainqêntanglha, which reaches elevations of up to 7000 m asl. This catchment exhibits the largest altitudinal gradient. One major stream drains the meltwater of both the Genpu and Zhadang glaciers. The steep relief of the Qugaqie catchment provides a section through all vegetation zones. Sparsely vegetated glacial foreland defines large parts of the catchment at higher elevations (Fig. 2d). Alpine wetlands are found in depressions. The dominant vegetation type is *K. pygmaea* pasture, which is used for yak grazing in the summer.

The Zhagu catchment is the smallest catchment (46 km^2) with limited altitudinal differences (peak at 5230 m asl.). Two stream systems drain the catchment (Fig. 2b), but the catchment was arheic during the investigation, only episodic drainage events into the lake occur. The stream water is sourced by groundwater springs and precipitation (Tran et al., 2021). The catchment has intense signs of degradation of the pasture biome, visible through barren soil and isolated patches of alpine pasture turfs (so called pancake-land; Miehe et al., 2019). Animal husbandry is concentrated around the stream beds and the flanks of hills.

2.2. Water sampling

Samples of stream and lake water were collected during three field campaigns in June/July 2018, May 2019, and September 2019 to cover seasonal differences. No samples were collected in May 2019 in the Qugaqie catchment due to weather conditions. The sampling scheme was designed to cover the influence of terrestrial endmembers. Glacial effluents were collected in Niyaqu ($n = 7$) and Qugaqie ($n = 6$), an extended wetland in the Niyaqu catchment was sampled ($n = 2$), groundwater springs samples were collected in the Zhagu catchment ($n = 8$). An overview of all water samples is given in Fig. 1, while endmember affiliations are depicted in the supplementary materials (Fig. S1). Further samples were taken from the course of the streams in Niyaqu ($n = 61$), Qugaqie ($n = 20$) and Zhagu ($n = 15$) to cover changes in DOM composition from the source until the river mouth (Fig. 2).

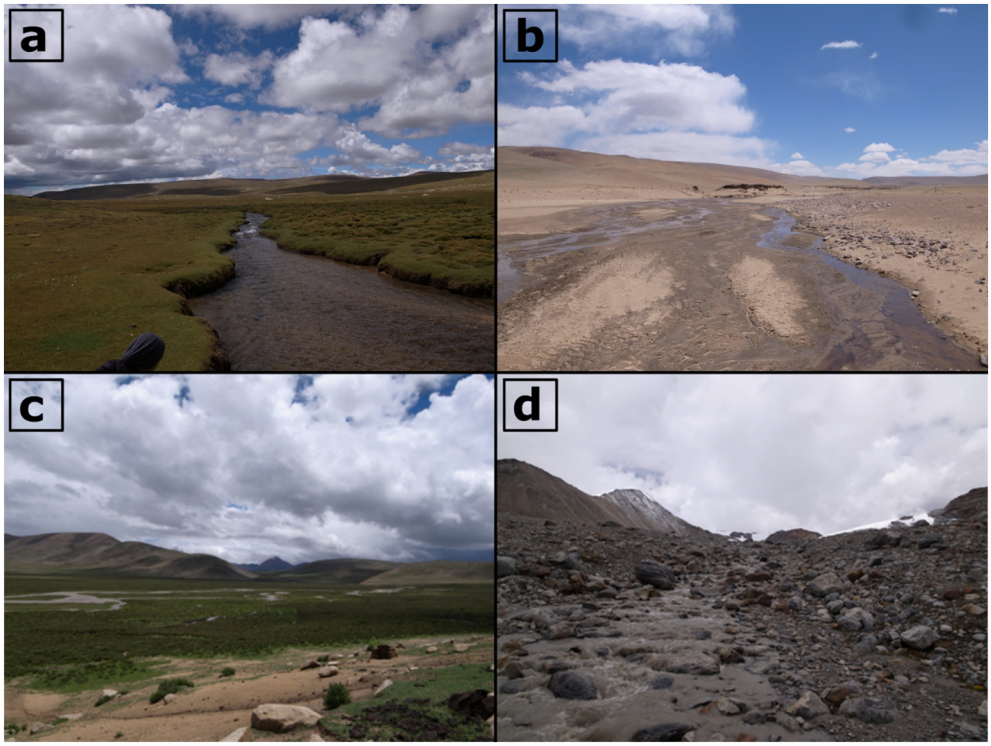

Fig. 2. Landscape units of the sampling area. a: *Kobresia pygmaea* turfs in the Niyaqu catchment. b: Periodical stream in the Zhagu catchment alpine steppe. c: Alpine wetland in depression of the Niyaqu catchment, in the foreground degraded, south-exposed hillslope. d: Glacial foreland of Zhadang glacier, Qugaqie catchment.

Samples of the lake (n = 8) and the brackish intermixing zones of the Niyaqu (n = 6) and Qugaqie catchment (n = 5) were taken. Samples of terrestrial endmembers (glacial, groundwater spring, wetland) were put into a composite group named 'sample category' together with stream samples and brackish and lake samples, allowing to differentiate these categories on watershed scale.

Mixed samples were collected (1 L was used from a 7 L mixed sample) from the middle depth of the pelagial in a central position of the stream in polyethylene bottles (HDPE). Mixed lake samples close to the shore were collected in the middle of the stream mouth from the pelagial, in 1 m depth and off-shore lake samples were taken about 200 m off shore from the studied catchments, as mixed samples at the surface and in 30 m depth using a submersible sampler. In addition, groundwater samples, used for $\delta^{13}C$ of DOM, were obtained in May 2019 from piezometers of the Zhagu catchment (Fig. 1) as described by Tran et al. (2021).

Prior to sampling, bottles were rinsed with 10% HCl, washed with ultrapure water and dried. After sampling 350 μg L^{-1} $HgCl_2$ was added to the samples to inhibit biological degradation (VDLUFA, 2012). All samples were kept at −21 °C until analysis.

2.3. Soil, sediment and plant samples

To track potential source materials of riverine DOM, $\delta^{13}C$ of C_{org} was measured in topsoil material (n = 15), collected in six locations of the Niyaqu catchment (Fig. 1). Glacial sediment (n = 3), was sampled on the Zhadang glacier in the Qugaqie catchment. Samples of *K. pygmaea* root (n = 4) and a shoot of a water plant (*Elodea*) (n = 4), were taken in the Niyaqu catchment and wetland, respectively (Fig. 1).

2.4. Sample analyses

Water samples were filtered using a 0.45 μm polyethersulfone (PES) membrane (Supor, Pall, Port Washington, USA). pH was measured at 20 °C using a potentiometric glass-electrode, calibrated with three standard solutions at pH 4.01, 7.00 and 10.01 (DIN 19266:2015–05). Electrical conductivity (EC) was determined using a conductivity sensor at 20 °C, controlled with a standard solution (0.01 mol $^{-1}$ KCl) (DIN EN 27888:1993–11). The concentration of cations Na^+, Mg^{2+}, Ca^{2+}, K^+, Li^+, and NH_4^+ and anions Cl^-, SO_4^{2-}, PO_4^{3-}, NO_2^-, NO_3^-, F^-, Br^-, and $(COO)_2^{2-}$ were analysed by ion chromatography (Metrohm 930 Compact IC Flex, Herisau, Switzerland).

DOC concentrations were determined by high-temperature oxidation in 20 mL aqueous samples, acidified with 50 μL of 32% HCl in a total organic analyzer (varioTOC Cube, Elementar, Langenselbold, Germany). Total dissolved carbon (TDC) samples were treated similarly, but no acid was added, dissolved inorganic carbon (DIC) was calculated.

The $\delta^{13}C$ values of DOM samples were measured in solution after acidification with HCl (32%) to pH 2 in an isoTOC cube (Elementar, Langenselbold, Germany) coupled with a continuous flow isotope ratio mass spectrometer (Elementar, Langenselbold, Germany; Federherr et al., 2014; Kirkels et al., 2014; Leinemann et al., 2018). When the DOC concentration was below 1.6 mg C L^{-1}, 1 mL of caffeine standard (reference material IAEA-600) was added. Sample $\delta^{13}C$ was calculated using the common mixing equation.

In addition, $\delta^{13}C$ was measured in potential source materials of riverine DOM. This included glacial sediment, topsoil samples and plant samples of *K. pygmaea* and *Elodea*. All samples were dried at 40 °C until a constant weight was reached. Samples were sieved to <2 mm equivalent diameter and milled. Inorganic carbonate was destroyed using the volatilization method (Hedges and Stern, 1984; Harris et al., 2001). $\delta^{13}C$ of organic carbon was determined using a isoprime cube elemental analyzer (Elementar, Langenselbold, Germany) coupled with an isoprime 100 isotope ratio mass spectrometer (Elementar, Langenselbold, Germany).

Ultraviolet absorbance properties of aqueous samples were determined using a Spectro Star Nano device (BMG Labtech, Ortenberg, Germany) with a 1 mL Suprasil® cuvette in temperature-controlled conditions (20 °C), scans were blank corrected. The UV/VIS absorbance at 254 nm ($SUVA_{254}$) was normalized by the DOC content (Weishaar et al., 2003). Absolute absorbance values at 254 nm (A254) were taken uncorrected.

Fluorescence of DOM (FDOM) was measured using an Edinburgh F920 spectrometer (Edinburgh Instruments, Livingston, UK). Measurements were conducted in temperature-controlled conditions (20 °C), in 90°mode in a QX class Suprasil® 300 cell with a path length of 10 mm. Excitation modes were set to 280–450 nm with a 5 nm step width and emission was set between 350 and 600 nm with 2 nm step width. Integration time was defined as 0.1 s and slit width (Δλ) was set to 10 nm in both the excitation and emission mode. An ultra-pure water Raman standard was used to avoid hysteresis effects. Further information about the technical application of parallel factor analysis (PARAFAC) on excitation-emission-matrices (EEMs) can be found in the supplementary materials.

EEMs were corrected with 95% of a blank process sample to remove the water Raman signal. PARAFAC was run using the N-way toolbox (Andersson and Bro, 2000) in MATLAB R2017b (The MathWorks, Natick, USA). The dataset was found to be very diverse with large differences between sampling points. To prevent confoundation due to concentration induced mode shifts, we conducted PARAFAC in a twofold approach. First, a subprime 4 component PARAFAC model was estimated and factor scores were summed for each sample. A threshold of $5*10^5$ relative concentration was determined to split the dataset into two more homogeneous datasets. Second, PARAFAC was then run for each group, i.e. low fluorescence response (below the threshold) and high fluorescence response (above the threshold). Sample group affiliation is depicted in the supplementary materials (Fig. S5-S7). Residual mean EEMs of both models are depicted in the supplementary materials (Fig. S2, S3). Resulting fluorescence components were statistically correlated to the variables of the multiparameter dataset using bivariate regression and compared with published FDOM components using the OpenFluor database (Murphy et al., 2014). Identification of the FDOM marker function was done by assigning the components to one of two groups indicating sources: a) microbial or protein-like DOM sources that form as the result of microbial activity and b) components forming a group addressed as terrestrial-like substances, such as lignin, polyphenols and tannins or resynthesized compounds, rich in phenols, deriving from the formation of soil organic matter (Fellman et al., 2010).

2.5. Plant coverage estimates

Plant cover estimates (PCE) were calculated using pre-trained support vector machine regression (SVE) models, published in Lehnert et al. (2015a). Three different models have been used which were exclusively trained for multispectral satellite data acquired by Landsat 5, 7, and 8. Therefore, no harmonization was required as suggested e.g., by Roy et al. (2016). The models have been validated against field samples from the Tibetan Plateau (Overall RMSE = 7.13, RMSE values of sensor specific models 3.95 (Landsat 8), 7.01 (Landsat 7) and 7.54 (Landsat 5), for details see Lehnert et al., 2015b). Scenes of Landsat 5, 7, and 8 for the last 30 years were used to receive plant cover maps of the whole Nam Co watershed with 30 m spatial resolution. Landsat scenes were downloaded from the United States Geological Survey website (http://earthexplorer.usgs.gov) and processed using an extended version of the 6S-code for atmospheric corrections (Curatola Fernández et al., 2015; Vermote et al., 1997) and the Minnaert model for topographic corrections (Riano et al., 2003). Obstructions (e.g., clouds) were removed using the quality bands of the Landsat data. In total, 24 watershed-wide acquisitions were available for the plant cover assessment. Pixel-wise mean and standard deviations (SD) of plant coverage were calculated for the investigation period. The final product shows a good conformity with the actual plant cover of our study area and was cross-verified by field investigations. Non-parametric Mann-Kendalls correlation tests were applied to those pixels where at least 7 valid PCEs were available (significance level of $\alpha \leq 0.05$). These tests were applied to detect changes of plant cover over time (decreasing or increasing). The term greening is used for significant increases of plant cover. For the processing of the satellite data including the plant coverage estimates, R (The R project for statistical computing, v3.6.3, GNU free software) was used.

Differences in the mean plant cover of the investigated catchments Niyaqu, Qugaqie, and Zhagu were compared by the non-parametric Conover-Iman test using the R-package 'conover.test' (Dinno, 2017) with significance level of $\alpha \leq 0.05$. Bonferroni post-hoc correction was applied using the R-base package (R Core Team, 2013).

2.6. Statistics

The dataset was grouped into three main effects: (I) site (i.e. catchments and lake), (II) sample category including endmembers (i.e. glacial effluents, groundwater springs and wetland water) as well as all stream samples and lake and brackish waters and (III) seasons. Mean and SD were calculated for sites, sample categories and seasons. To gain information about watershed-wide seasonal effects, mean values were calculated as a composite from all three catchments. Watershed-wide mean composites of streams were compared to other sample categories including endmember classes to reveal the degree of variation within this effect group. Non-parametric tests and comparisons between and within the main effect groups were conducted. Since prerequisites for parametric tests could not be met, we conducted non-parametric tests: the Mann-Whitney-*U* test for pairwise comparisons and Conover-Iman test for multiple pairwise comparisons of repeated measurements, using Bonferroni post-hoc correction. Significant effects were accepted on the level of $\alpha \leq 0.05$. Multiparameter subsets were created by connecting the DOM and water chemistry dataset with PARAFAC-resolved FDOM components. Multiple bivariate regressions and non-metric multidimensional scaling (NMDS) were performed. NMDS is classically used to compute the ecological distance or β-diversity between samples (Faith et al., 1987; Anderson et al., 2006). We applied this distance approach to calculate the biogeochemical distance between samples. NMDS was performed on mean-centred and scaled data, using the vegan package (Oksanen et al., 2020). For the first subset, including the high fluorescence response FDOM data, the Euclidean dissimilarity index and $k = 3$ was used. The Manhattan index and $k = 3$ was used for the low fluorescence response FDOM components and corresponding dataset, forming the second subset. Tables of scores, coefficients of determination (R^2) (Table S4, S5) and of loadings (Table S6) are provided in the supplementary materials.

Statistics were computed using R (The R project for statistical computing, v3.6.3, GNU free software), its base packages (R Core Team, 2013), the 'tidyverse' meta-package, (Wickham et al., 2019) and 'conover.test' (Dinno, 2017) for the Conover-Iman test.

3. Results

3.1. Plant coverage estimates around Lake Nam Co

The mean plant cover in the Nam Co watershed area was 48.1 % for the investigated period. In the three investigated catchments, PCE decreased in the order Niyaqu (52.3%) > Qugaqie (49.5 %) > Zhagu (44.5 %) (supplementary materials Table S1). The vegetation cover showed an altitudinal- and exposition- dependent distribution with more green plant cover in the south-west and east of the Nam Co watershed compared to the north and north-west (Fig. 3a). Plant cover was connected with water availability and increased insulation (north exposition) during the dry season. Especially the northern exposed valleys of the Nyainqêntanglha showed an overall higher plant cover driven by the water surplus received from glacial meltwater (Song et al., 2014). The western catchments were characterized by high plant cover along streams and in depressions, while the southern exposed slopes in the northern Nam Co watershed exhibited low plant cover of 35 to 45 %. The satellite based PCE data are consistent with field surveys in the catchments, which revealed wetlands with mires and submerged plants (*Elodea*) and of vast *K. pygmaea* pastures close to streams and on insulated hill slopes mostly with an east-west valley course. Alpine pastures are partly an azonal vegetation type in our study area, because *K. pygmaea* covered the river banks almost to the lake (Fig. 3a).

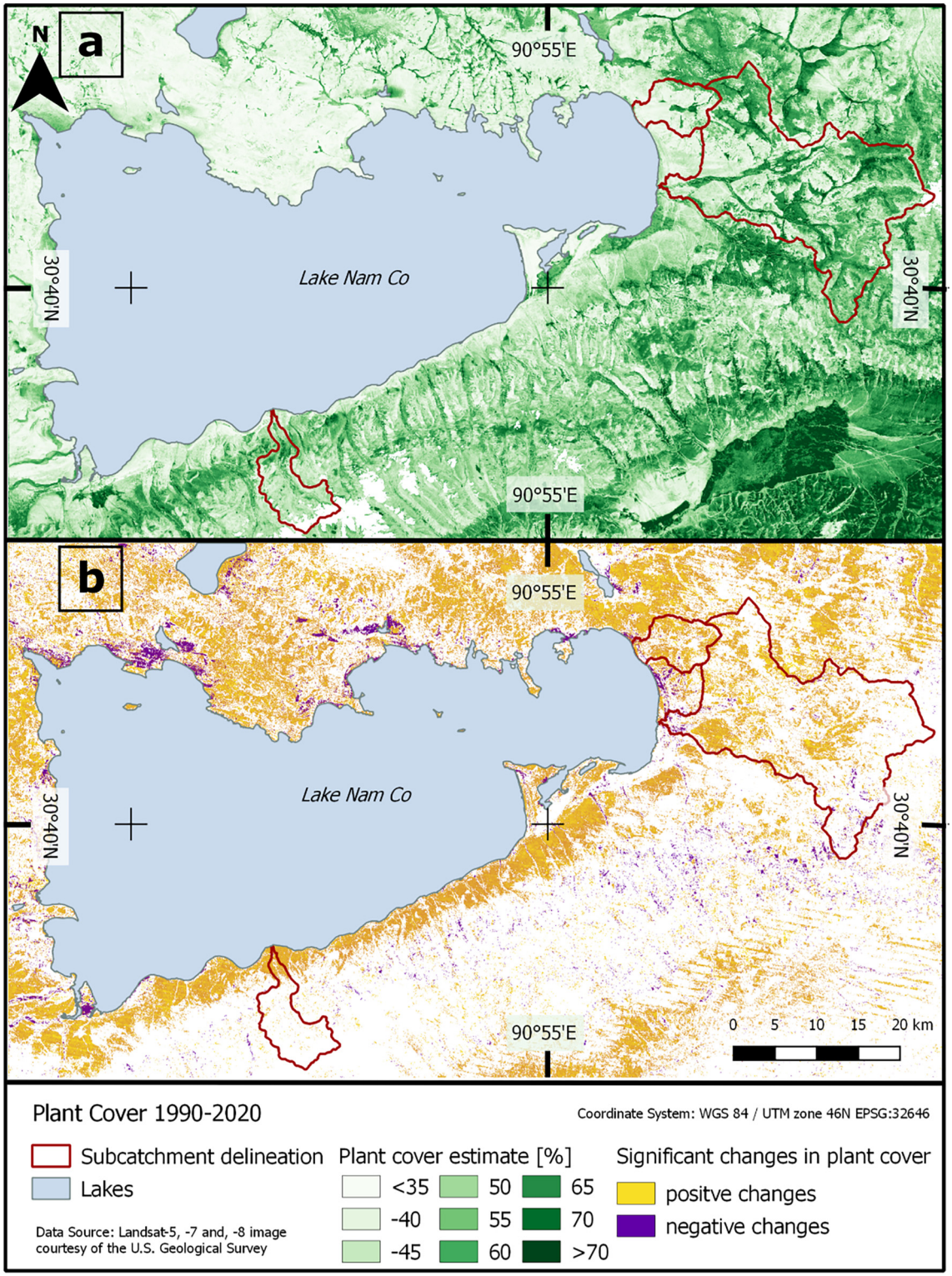

Fig. 3. Mean plant cover estimate (PCE) for 1990–2020 in 30 m resolution (a) and significant changes during the investigation period (b).

During the 30-year investigation period, only a small number of pixels revealed a significant decrease in plant cover, corresponding to 3.9 % of the depicted watershed area, whereas in large areas a pronounced greening was observed, this comprised approximately 28.2% of the investigated watershed area (Fig. 3b). Especially the southern shoreline and the eastern and north-eastern areas of the Nam Co watershed exhibited a significant greening trend between 1990 and 2020.

3.2. Solute composition in the catchments and Lake Nam Co

Water pH values from Lake Nam Co were different in comparison to stream water in the three catchments (Fig. 4a, Table 1). Differences also existed between water samples from Niyaqu > Qugaqie and between Qugaqie < Zhagu (Table 1). Samples from June/July 2018 showed higher pH values than those from May 2019 and September 2019. Glacial effluents

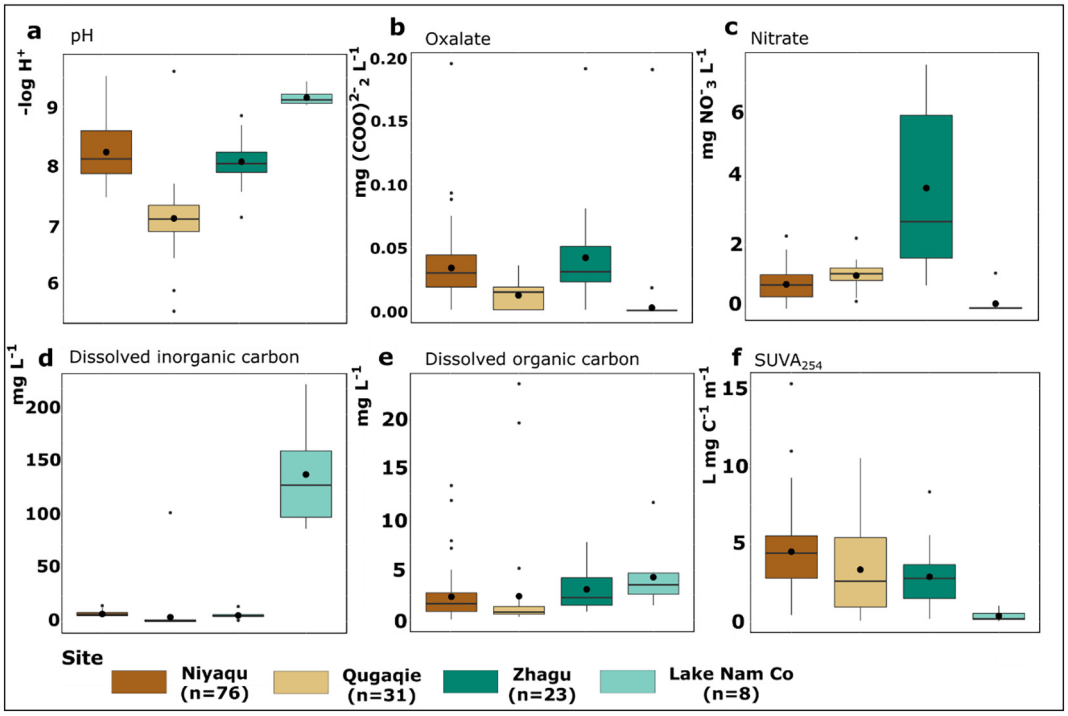

Fig. 4. pH (a), oxalate (b), nitrate (c), DIC (d), and DOC (e) concentrations, and $SUVA_{254}$ values (f) of stream waters from Niyaqu, Qugaqie, Zhagu catchments and Lake Nam Co. Large black dots show the mean, horizontal lines show the median and whiskers are defined as respective quartile (I/III) +/− 1.5*inter-quartile range, outliers are shown as small black dots.

had the lowest pH compared to stream samples (Table 2). Mineral nitrogen concentrations also varied in the catchments. Ammonium showed smaller concentrations in the June/July 2018 sampling season compared to May 2019 (Table 1), while wetland water showed highest values compared to the other sample categories (Table 2). Water samples of the Zhagu catchment showed highest nitrate concentrations, followed by Qugaqie and Niyaqu. The lake showed the lowest nitrate concentration (Fig. 4c). Seasonal effects on nitrate were visible, with May 2019 samples showing higher values compared to June/July 2018 and September 2019. Nitrate concentrations were higher in water samples collected from springs compared to lake and brackish water, glacial effluents and wetland water samples (Table 2).

The Niyaqu and Zhagu stream samples had higher calcium concentrations compared to those of Qugaqie stream and Lake Nam Co (Table 1). Differences were found between calcium concentrations in stream samples and wetland water compared to lake and brackish water samples, with the latter showing higher concentrations. The results for a large group of anions and cations showed a similar pattern. Along with EC and DIC concentration, bromine, lithium, chlorine, fluorine, magnesium, potassium, sodium and sulphate had the highest concentrations in Lake Nam Co samples compared to the three investigated catchments. The differences were also observable for the following sample categories: wetland waters, water from springs and glacial effluents along with stream water had lower concentrations than lake and brackish water samples (Table 2). The

Table 1
Solute composition for stream water samples from the Niyaqu, Qugaqie, and Zhagu catchments and from Lake Nam Co, and at different seasons of all three catchments, i.e. at Indian summer monsoon (June/July 2018), at freshet (May 2019), and at base flow (September 2019 = Sep 2019). Shown are arithmetic means and standard deviation (SD).

Variable	Niyaqu		Qugaqie		Zhagu		June/ July 2018		May 2019		Sep 2019		Lake Nam Co	
	Mean	*SD (±)*	*Mean*	*SD (±)*	*Mean*	*SD (±)*	*Mean*	*SD (±)*	*Mean*	*SD (±)*	*Mean*	*SD (±)*	*Mean*	*SD (±)*
pH	8.23	0.49	7.11	0.65	8.06	0.38	9.41	0.13	8.24	0.94	7.90	0.41	7.88	0.70
EC [µS cm^{-1}]	112.33	33.81	80.70	206.70	105.11	32.23	1457.5	301.38	207.68	376.64	136.05	214.57	190.17	377.92
NH_4^+ [mg L^{-1}]	0.00	0.03	0.00	0.00	0.01	0.01	0.01	0.01	0.00	0.01	0.00	0.01	0.00	0.04
NO_3^- [mg L^{-1}]	0.77	0.50	1.05	0.41	3.75	2.45	0.17	0.38	1.06	1.26	1.87	1.99	1.12	1.35
Ca^{2+} [mg L^{-1}]	9.43	4.10	3.94	1.41	8.06	2.63	2.15	0.52	6.74	4.02	7.55	3.78	8.33	4.51
Br^- [mg L^{-1}]	0.00	0.00	0.00	0.03	0.00	0.00	0.21	0.05	0.01	0.05	0.00	0.03	0.01	0.06
Li^+ [mg L^{-1}]	0.00	0.00	0.00	0.04	0.00	0.00	0.28	0.14	0.02	0.08	0.00	0.00	0.02	0.09
Cl^- [mg L^{-1}]	2.68	1.77	3.92	7.25	3.28	1.95	50.57	13.70	8.29	12.30	4.08	8.65	4.70	13.88
F^- [mg L^{-1}]	0.05	0.03	0.23	0.50	0.06	0.01	3.80	0.48	0.42	1.04	0.16	0.59	0.32	0.95
Mg^{2+} [mg L^{-1}]	1.88	0.80	1.53	5.99	1.49	0.48	52.17	9.93	5.49	12.64	3.08	9.74	4.97	13.87
K^+ [mg L^{-1}]	0.59	0.23	1.10	3.58	1.15	0.49	26.01	6.95	2.75	6.68	1.49	4.42	2.37	7.21
Na^+ [mg L^{-1}]	2.24	1.29	7.16	33.98	3.33	1.06	234.86	57.66	22.06	62.49	9.33	42.93	17.65	63.30
SO_4^{2-} [mg L^{-1}]	12.53	11.02	10.17	22.66	2.78	0.96	160.42	39.72	21.49	40.85	13.08	29.87	20.71	42.79
PO_4^{3-} [mg L^{-1}]	0.00	0.01	0.00	0.00	0.01	0.03	0.01	0.02	0.00	0.01	0.06	0.02	0.00	0.01
$(COO)_2^{2-}$ [mgL^{-1}]	0.03	0.02	0.01	0.01	0.04	0.03	0.01	0.01	0.03	0.02	0.02	0.03	0.02	0.02
DIC [mg L^{-1}]	7.60	2.32	4.54	18.75	6.26	2.68	141.63	51.13	16.41	34.80	8.24	13.84	16.92	44.47
DOC [mg L^{-1}]	2.22	2.26	2.28	5.18	2.94	2.09	4.31	3.21	3.10	4.27	1.87	2.21	2.30	2.40
$SUVA_{254}$ [L mg C^{-1} m^{-1}]	4.47	2.56	3.32	2.93	2.87	1.79	0.39	0.37	1.70	1.33	5.52	2.92	4.37	2.16

Table 2
Solute composition of different sample categories, of all studied streams and the lake. Shown are arithmetic means and standard deviation (SD). Fluorescence components are in the unit of relative intensity (RI).

Variable	Stream water		Glacial effluent		Spring water		Wetland water		Lake and brackish water	
	Mean	*SD (±)*	*Mean*	*SD (±)*	*Mean*	*SD (±)*	*Mean*	*SD (±)*	*Mean*	*SD (±)*
pH	7.99	0.63	7.29	0.91	8.05	0.56	8.14	0.27	8.68	0.88
EC [μ S cm^{-1}]	96.21	38.07	74.82	51.80	105.14	51.02	171.85	1.91	722.28	715.96
NH_4^+ [mg L^{-1}]	0.00	0.01	0.01	0.01	0.01	0.02	0.17	0.21	0.01	0.01
NO_3^- [mg L^{-1}]	1.35	1.53	0.88	0.60	3.37	2.62	0.04	0.01	0.61	0.50
Ca^{2+} [mg L^{-1}]	8.16	3.99	6.91	4.88	7.73	3.54	14.09	2.86	4.16	2.91
Br^- [mg L^{-1}]	0.00	0.00	0.00	0.00	0.00	0.00	0.00	0.00	0.10	0.11
Li^+ [mg L^{-1}]	0.00	0.00	0.00	0.00	0.00	0.00	0.00	0.00	0.13	0.17
Cl^- [mg L^{-1}]	3.02	1.90	2.00	1.42	2.42	1.95	2.10	1.47	24.54	25.96
F^- [mg L^{-1}]	0.08	0.05	0.04	0.02	0.06	0.01	0.24	0.01	1.83	1.86
Mg^{2+} [mg L^{-1}]	1.48	0.74	1.34	1.23	1.13	0.47	4.55	0.32	24.48	26.09
K^+ [mg L^{-1}]	0.67	0.39	0.46	0.25	0.68	0.38	1.30	0.21	12.39	13.45
Na^+ [mg L^{-1}]	2.25	1.27	0.65	0.35	2.58	1.16	4.72	0.59	110.23	122.48
SO_4^{2-} [mg L^{-1}]	9.64	10.00	12.29	10.98	1.98	0.80	2.95	0.04	79.39	80.00
PO_4^{3-} [mg L^{-1}]	0.00	0.02	0.00	0.00	0.01	0.04	0.04	0.06	0.01	0.02
$(COO)_2^{2-}$ [mgL^{-1}]	0.03	0.03	0.01	0.01	0.03	0.01	0.12	0.10	0.01	0.02
DIC [mg L^{-1}]	6.04	3.09	3.66	3.38	6.27	2.85	14.58	1.56	67.83	75.61
DOC [mg L^{-1}]	2.41	3.23	0.63	0.46	2.84	2.13	12.46	1.04	2.89	2.60
Absorbance [254 nm]	0.06	0.05	0.03	0.02	0.10	0.09	0.34	0.00	0.04	0.02
$SUVA_{254}$ [L mg C^{-1} m^{-1}]	3.94	2.60	4.90	2.79	3.45	2.39	2.70	0.23	2.01	2.58
$\delta^{13}C$ of DOM [‰]	−24.85	3.48	−24.21	6.46	−24.22	4.81	−25.50	0.54	−23.21	3.84
FC 1 (high) [RI ∗ 10^6]	3.46	0.22	0.25	0.04	0.40	0.35	1.28	0.28	0.20	0.08
FC 2 (high) [RI ∗ 10^5]	2.05	1.44	1.57	0.21	2.87	2.63	6.04	1.38	1.15	0.39
FC 3 (high) [RI ∗ 10^5]	0.75	2.55	0.15	0.02	0.17	0.16	1.67	1.00	0.27	0.15
FC 4 (high) [RI ∗ 10^5]	1.29	1.07	1.04	0.14	1.75	1.74	5.00	1.46	0.90	0.32
FC 1 (low) [RI ∗ 10^4]	6.77	3.55	2.41	2.37	5.68	0.78	n.d.	n.d.	4.59	3.21
FC 2 (low) [RI ∗ 10^4]	4.96	3.26	1.37	1.69	3.68	1.36	n.d.	n.d.	3.31	2.25
FC 3 (low) [RI ∗ 10^4]	2.11	2.91	0.73	0.62	0.87	0.23	n.d.	n.d.	2.02	2.76
FC 4 (low) [RI ∗ 10^4]	1.53	0.86	2.31	5.54	1.38	0.10	n.d.	n.d.	1.01	0.72

comparison of DIC concentrations showed different results between glacial effluents and wetland water samples with higher concentrations (Table 2). Phosphate concentrations differed not only between the catchments and the lake, but also between the streams, where samples of the Zhagu catchment had larger values than those of Niyaqu and Qugaqie.

Lake Nam Co water samples showed smaller oxalate concentrations than stream samples from the Niyaqu and Zhagu catchments. Smallest oxalate concentrations were measured in Qugaqie samples, (Fig. 4b, Table 1). In sample categories, oxalate concentrations were increased in wetland water and stream water compared to samples from lake and brackish, and glacial sources (Table 2). With regard to seasons, oxalate concentrations were increased in June/July 2018 compared to May 2019, and September 2019.

DOC concentrations in water samples of the three catchments and Lake Nam Co varied between 0.1 and 23.2 mg L^{-1} (Fig. 4e, Table 1). Mean DOC concentrations were 4.3 mg C L^{-1} in water samples from Lake Nam Co and higher compared to Niyaqu (2.2 mg C L^{-1}) and Qugaqie (2.3 mg C L^{-1}), while the mean DOC concentration of the Zhagu catchment (2.9 mg C L^{-1}) showed no differences. Wetland waters showed highest DOC concentrations (12.4 mg C L^{-1}), while glacial waters showed significantly lower concentrations (0.6 mg C L^{-1}), both compared to other sample categories (Table 2).

The specific ultraviolet absorbance of DOM at 254 nm ($SUVA_{254}$) revealed significant differences between catchments, sample categories and seasons (Fig. 4f, Table 1, Table 2). First, lake samples had lower absorbance values compared to the stream water samples from all three catchments. Second, catchment $SUVA_{254}$ increased in the order Zhagu < Qugaqie < Niyaqu, but was significantly different between Zhagu and Niyaqu only. Stream water and glacial effluents had higher $SUVA_{254}$ values compared to lake and brackish water samples. For sample categories $SUVA_{254}$ decreased in the order glacier > stream > spring > wetland > brackish/lake, while absolute absorbance (A254) was highest in wetland waters and significantly different compared to glacial effluents and lake and brackish waters (Table 2). Samples taken in June/July 2018 had lower $SUVA_{254}$ than the May and September 2019 samples (Table 1).

$\delta^{13}C$ values of DOM in soil and groundwater were only slightly less negative compared to those in plants (Fig. 5). In contrast, organic materials in glacial sediments were more enriched in ^{13}C compared to all other samples. The stream samples of the Qugaqie catchment, receiving glacial meltwater, were characterized by less negative $\delta^{13}C$ values of DOM. Also DOM from brackish zones and Lake Nam Co was enriched in ^{13}C (Table 2). Water of sample categories showed differences, but these were not significant. Wetland water showed the most depleted $\delta^{13}C$ of DOM compared to other sample categories (Table 2). $\delta^{13}C$ values in lake samples were different in comparison to those of soils, plants, and groundwater as well as from water samples from the Zhagu and Niyaqu catchments, which form a first statistical group, except for the June/July 2018 samples (Fig. 5). Riverine DOM from the Qugaqie catchment, from Niyaqu and Zhagu during the monsoon season, glacial sediments and lake DOM belong to a second statistical group. With respect to strong seasonality, $\delta^{13}C$ of DOM of riverine samples taken in June/July 2018 were different from those taken in May 2019 and September 2019 (Fig. 5).

3.3. PARAFAC resolved fluorescence spectroscopy EEMs

Two PARAFAC models were produced from the fluorescence EEMs, one for the high fluorescence response subset and one for the low fluorescence response subset. Detailed model descriptions and graphical visualisations can be found in the supplementary materials (Fig. S4). The high fluorescence response model consists of four components, FC 1 with excitation/emission maxima [nm] of (320/425), FC 2 (280/500) with a second excitation peak at 405 nm, FC 3 (280/350) and FC 4 (360/465). A set of $n = 78$ samples is described. Analysis of sample factor loadings revealed unique contributions of all modelled components for the samples, component loadings are statistically different from each other on a level of $\alpha \leq 0.05$ (Pearson correlation coefficient). The low fluorescence response model showed a

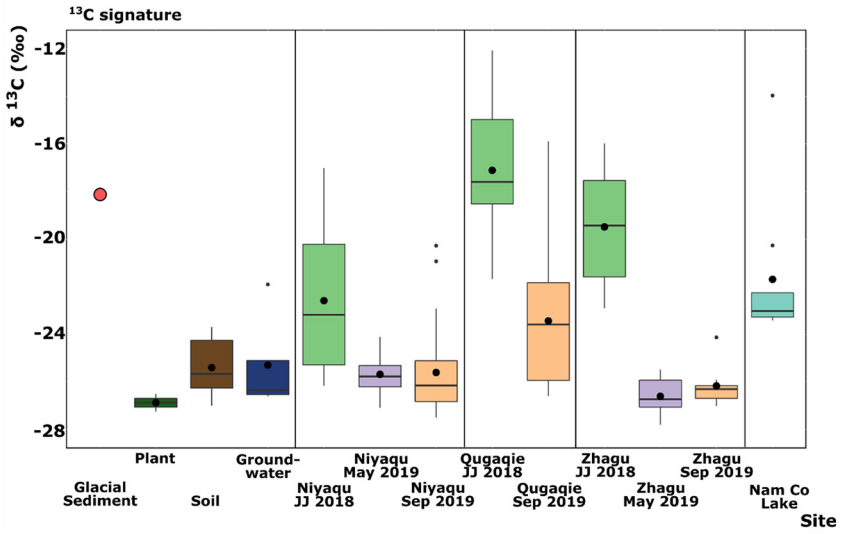

Fig. 5. $\delta^{13}C$ natural abundance signatures of stream and lake DOM of the Nam Co watershed, along with its potential source material: glacial sediments (expressed as dot / $n = 3$ with standard deviation < size of the symbol), plants, topsoils, and groundwater. Boxplots depictions is as follows: large black dots show the mean, horizontal lines show the median, and whiskers are defined as respective quartile (I/III) +/− 1.5*inter-quartile range, outliers are shown as small black dots. Abbreviations are: JJ = June/July, Sep = September; no sampling was possible in May 2019 in the Qugaqie catchment.

four component solution to describe the set of $n = 61$ samples. Excitation and emission maxima of components are FC 1 (330/430), FC 2 (390/475), FC 3 (280/350) and FC 4 (280/420). In the low subset, FC 3 and FC 4 are positively correlated. All other components of the low fluorescence response model are not statistical related (Pearson correlation coefficient, $\alpha \leq 0.05$).

3.4. Bivariate regression and NMDS ordination of the PARAFAC resolved FDOM components with the combined DOM dataset

Characteristics of FDOM components were tested against variables of the DOM and water chemistry dataset (supplementary materials Table S2). For the high fluorescence response components, if not stated differently, reported relations were positive. Interpretations were further tested using already published fluorescence spectra using the OpenFluor database (Murphy et al., 2014) reported in detail in the supplementary materials (Table S3).

Component FC 1 showed relationships to DIC, DOC, sodium, chloride, and magnesium, FC 2 has weak relationships with DIC, DOC, chloride, sodium and, magnesium, while the third FDOM component (FC 3) was correlated to potassium and nitrate and negatively correlated to $\delta^{13}C$ of DOM, with weak and very weak fits, respectively. The fourth component (FC 4) showed a weak regression trend with DIC, DOC, chloride, and magnesium concentration. FDOM components 1, 2 and 4 represented plant and soil-derived *terrestrial-like* fluorophores, the latter suggested lignin-phenols as FDOM source. These components were connected to solutes originating from plants or soil with reworked residues from the terrestrial domain. This was corroborated by comparisons in the OpenFluor database. Component FC 3 represents a *microbial-like* FDOM component. Here, protein-derived tryptophan was indicated as FDOM source.

For the low fluorescence response subset, a positive relationship was identified between FC 1 and the $\delta^{13}C$ ratio of DOM, FC 2 revealed weak positive correlations with $\delta^{13}C$ of DOM and calcium concentration. The third FDOM component showed a negative correlation with $SUVA_{254}$ and a positive correlation with $\delta^{13}C$ of DOM, while FC 4 was weakly positive correlated with ammonium and $SUVA_{254}$. FDOM component 1 was interpreted as microbial-like fluorophore and FC 3 was identified as tyrosine, of an autochthonous protein-bound origin, corroborated by comparison with the OpenFluor database. FC 2 and FC 4 were identified as terrestrial-like fluorophores.

FDOM components (Fig. 6) were statistically compared in sites, sample category and seasons and taken as dependent variables in NMDS ordination (Fig. 7). For the high subset, the Qugaqie catchment had significantly lower FDOM concentrations compared to the Niyaqu and Zhagu samples for all terrestrial-like components (FC 1, FC 2, FC 4), being in-line with observed lower DOC concentrations, whereas the microbial-like component FC 3 was significantly increased in samples from Qugaqie (Fig. 6a). For the low fluorescence response subset, the relative concentration of FDOM components showed significant differences between the Qugaqie and Zhagu catchment, with the latter samples significantly higher in microbial-like FC 1 and terrestrial-like FC 2 and FC 4. Water samples from the lake were significantly lower in terrestrial-like FC 4 and microbial-like FC 1 compared to DOM from the Zhagu catchment (Fig. 6c).

For sample categories, all wetland samples were located in the high response subgroup. Here, the terrestrial-like FDOM component FC 1, and the microbial-like component FC 3 showed a trend of higher concentrations compared to all other sample categories (Table 2). The wetland samples, were exempt from statistical testing, due to the low sample size ($n = 2$). In the low fluorescence response subset, differences were found for the microbial-like components: FC 1, FC 3 and the terrestrial-like FC 2. Stream water samples were significantly enriched compared to glacial effluents. Lake and brackish water samples were enriched in microbial-like FDOM (FC 3) compared to glacial effluents, while glacial water had the highest overall values of a terrestrial-like FDOM in the low fluorescence response subgroup (FC 4) (Table 2).

Seasonal differences were visible for FDOM components of the high fluorescence response subset. Terrestrial-like FDOM components (FC1, FC 2 and FC 4) were significantly enriched during the baseflow season (September 2019) compared to freshet (May 2019) and the monsoon (June/July 2018). In contrast, microbial-like FDOM concentration of the high subset (FC 3) was significantly increased during the monsoon season compared to the other two seasons (Fig. 6b). In the low response subset, freshet FDOM was enriched in two components (FC 1 and FC 2) compared to samples drawn during the monsoon, while the microbial-like, tyrosine-like component FC 3 was significantly increased during monsoon compared to the other two seasons (Fig. 6d).

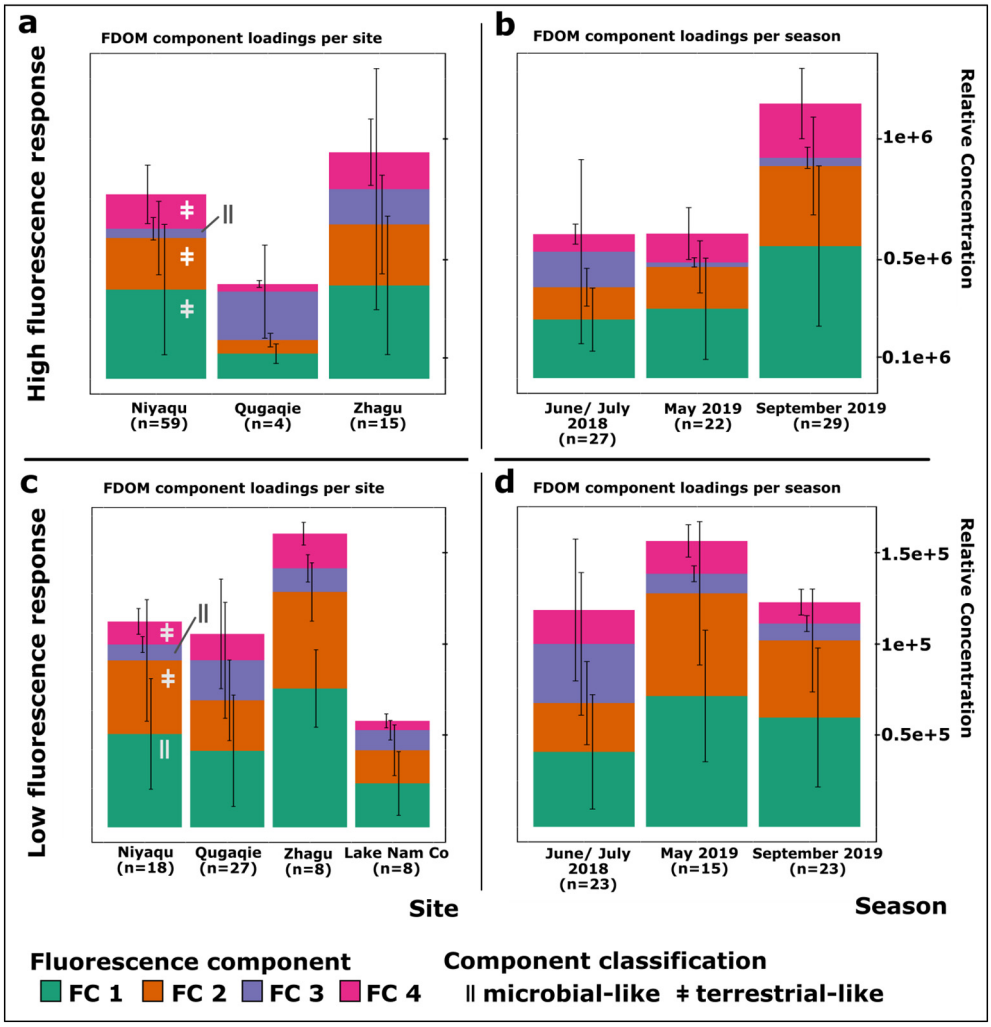

Fig. 6. Fluorescence DOM component loadings of the PARAFAC models for the high fluorescence response subgroup sites: a and seasons: b and for the low fluorescence response subgroup sites: c and seasons: d. Whiskers are defined by standard deviation. Note the scale offset between high and low subset.

The first NMDS ordination including the high fluorescence components of water samples is displayed in Fig. 7(a, b, c) for the three independent variables (site, sample category, and season, respectively). Dimension 1 of this ordination divided samples with high pH, high DIC and high EC readings. Terrestrial-like FDOM components (FC 1, FC 2 and FC 4) and DOC concentration defined this dimension as well. The negative direction of dimension 1 was driven by $\delta^{13}C$ of DOM. The second dimension for the first subset differentiated $SUVA_{254}$ and sulphate on the positive side and high concentrations of nitrate, oxalate, phosphate, potassium, DOC and microbial-like FC 3 (FDOM) on the negative side. When comparing the three catchments (Fig. 7a) and sample categories (Fig. 7b), samples from wetlands were strongly clustered in the positive direction of dimension 1. In contrast, samples from the Qugaqie catchment scored in a negative direction. At the second dimension, a separation of samples from the Niyaqu in the positive and the Zhagu catchment in the negative direction was apparent. For seasons, a scattering in ordination was visible (Fig. 7c). The June/July 2018 samples were mostly located in the negative directions of both dimensions, while the September 2019 samples were in the positive direction of the second dimension. Samples obtained in May 2019 were clustered in the core of the ordination space.

The second NMDS ordination contains the low response fluorescence FDOM components (Fig. 7d, e, f). The first dimension was explained by the DIC content, the EC readings, and by anions and cations. This direction was driven by a large group indicating the influence of salts and carbonates as well as EC and the DIC concentration. While $SUVA_{254}$ and the terrestrial-like FDOM component FC 4 were in the negative direction. $\delta^{13}C$ of DOM, ammonium and FDOM component FC 3 were positioned on the positive direction of the second dimension, while pH, nitrate, as well as oxalate, calcium, phosphate and two FDOM components (FC 1, FC 2) were in the negative direction. When examining clustering for sites, Lake Nam Co samples were separated from stream samples on the first dimension (the Qugaqie sample is close to the terminus), while the second dimension mostly resolved compositional differences between catchments. The Qugaqie and Niyaqu samples scored in the positive direction of dimension 2. The majority of the Zhagu samples scored in the negative space in both dimensions. The Lake Nam Co samples were not seasonally clustered, while the stream water samples of September 2019 scored more in the positive space of dimension 2 compared to the May 2019 samples, and June/July 2018 samples, those were spread in the ordination space (Fig. 7f).

4. Discussion

4.1. Plant cover

All three catchments revealed features of degradation but with different extents (Fig. 2b, c). The plant cover estimate (PCE) showed significantly lower plant cover in Zhagu and Qugaqie compared to the Niyaqu catchment. For the Zhagu catchment, we interpret this as a drought effect, caused by the absence of glacial meltwater and increasing aridity northwards, visible by lower MAP values. Intense animal husbandry in the remaining

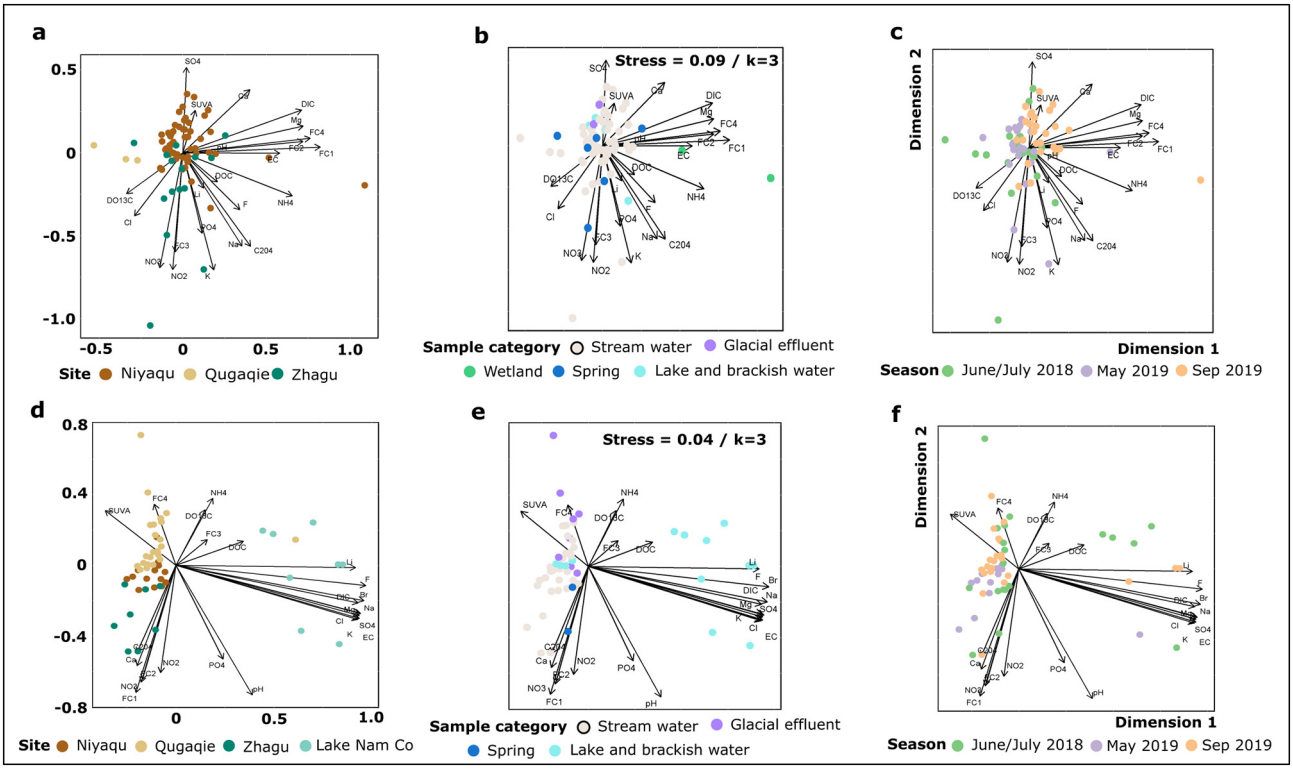

Fig. 7. Non-metric multidimensional scaling (NMDS) ordination plots for the multiparameter dataset including the high fluorescence response PARAFAC model, between sampling site a), sample category b), and sampling season c). NMDS ordination plots for the subset including the low fluorescence response PARAFAC model, between sampling site d), sample category e), and sampling season f). Note: NMDS dimensions are scaled to increase readability while loading vector length and direction are retained.

productive areas likely increases grazing pressure and leads to damaged pastures. The Qugaqie catchment, which is used as a summer pasture (Tibetan Pastoralists, 2019), is to a large extent covered with productive alpine pastures at lower altitudes. At the sub-nival to nival altitudinal zone, there is only sparse vegetation, leading to smaller watershed-wide mean PCE values compared to the Niyaqu catchment. In the Qugaqie catchment, the lower plant coverage is interpreted as a consequence of its high elevation.

Hopping et al. (2018) reported degraded pastures close to the southern shoreline of Lake Nam Co, which has also been found for *K. pygmaea* pastures at other locations on the TP (Damm, 1998; Qiu, 2016; Lehnert et al., 2016; Liu et al., 2018., Harris, 2010). In contrast, our satellite-based PCE estimate reveals only ~4 % of the land area with significant decrease of plant coverage during the last 30 years. In contrast, the PCE data confirmed a greening of the three catchment areas, in line with Zhang et al. (2008) and Zhong et al. (2019). But this cannot serve as a definitive evidence for the absence of degradation. Multispectral satellite data are feasible to detect changes in green cover, such as the loss of pasture patches, but are limited to track changes in species composition, which are important early warning signs for degradation (Miehe et al., 2008; Schleuss et al., 2015). In addition, the time series analysis of satellite data can only detect changes in ongoing degradation; an assessment of the degradation status is impossible without further environmental data. The large extent of plant cover increase in the Nam Co watershed is found mostly in areas with relatively low plant cover 30 years ago, which largely belong to the alpine steppe (Anslan et al., 2020), and most likely is due to the reported water surplus in the last decades (Zhang et al., 2019; Zhang et al., 2017). Greening and changes in plant cover can massively influence the formation of DOM (Singh et al., 2017). Our data show that high plant cover prevails along the course of the streams, according to field observations dominated by *K. pygmaea*.

4.2. Site-specific DOM signatures

The DOM signature in streams can vary strongly depending on the origin of DOM (Amon et al., 2012; Coch et al., 2019; Jaffé et al., 2012). Our data show that water biogeochemistry and DOM composition in streams of the three catchments and Lake Nam Co have unique signatures. They further differ between landscape units, reflecting different source areas such as wetlands and glacial ecosystems. In the following we discuss endmembers and landscape unit features from the three investigated catchments of the Nam Co watershed.

4.2.1. *K. pygmaea* pastures

Plant cover estimations show that the majority of stream water samples are directly influenced by *K. pygmaea*, even if embedded in an alpine steppe surrounding. The alpine pasture in the Qugaqie and Niyaqu catchment extends along the stream path almost to the stream terminus at Lake Nam Co. The majority of stream samples from Niyaqu and Qugaqie cluster together in a dimension influenced by high $SUVA_{254}$ (Fig. 7d), coinciding with high PCE in the surrounding (Fig. 3). The majority of stream banks are grown with *K. pygmaea* pastures. We identified significant conformity between high PCE and high $SUVA_{254}$ signatures (Kruskal-Wallis rank sum test; $\alpha \leq 0.05$). Further, correlations between high $SUVA_{254}$, depleted $\delta^{13}C$ of DOM and low DOC concentrations were identified, pointing towards a unique DOM signature in streams. The $\delta^{13}C$ ratios in DOM samples of streams (Table 2) are close to those of soil samples (Fig. 5), underlining a likely connection between terrestrial material and streams. Terrestrial-like FDOM components (high subset: FC 1, FC 2, FC 4; low subset: FC 4) in stream samples of Niyaqu and Qugaqie (Fig. 7a) also indicate a prominent influence of plant- and soil-derived materials and suggest a smaller share of in-situ microbial DOM production (e.g., by bacteria) in the stream. The latter is likely due to the short residence time of DOM in the fast-flowing streams, similar results were reported from a case study of low order streams from boreal Sweden (Kothawala et al., 2015).

Stream water DOM can contain large proportions of plant and soil derived components (Coch et al., 2019; Zhou et al., 2019). The prevailing *K. pygmaea* pasture is well understood to retain large amounts of water, nutrients and carbon in its root turfs (Kaiser et al., 2008; Schleuss et al., 2015), being likely responsible for the low DOC concentrations in stream water

samples. Further, the depleted $\delta^{13}C$ values and high $SUVA_{254}$ in these samples suggest a limited microbial processing of the terrestrial-borne DOM. Instead, a direct washing out of plant material into streams is probable. We conclude that alpine pastures lead to a unique DOM signature, controlled by the characteristics of the firm *K. pygmaea* root mat.

4.2.2. Glacial ecosystems

Glacial meltwater plays a key role for the water budget of the lake (Song et al., 2014). The hydrosphere of Niyaqu and the Qugaqie catchment are largely influenced by glacial meltwater (Gao et al., 2015). DOM from water samples taken at the glacial termini show unique DOM signatures. These water samples showed low DOC concentrations, high $SUVA_{254}$, despite sparse plant cover, and were richer in ^{13}C compared to DOM sampled downstream. This is accompanied by high concentrations of ammonium and the microbial-like FDOM component FC 4 (low fluorescence response dataset). We believe, that Tibetan glacier-derived DOM is chemically distinct from stream and lake DOM (Spencer et al., 2014; Li et al., 2021). Glaciers represent a unique environment with organic matter production by photoautotrophic microorganisms in-situ (Anesio et al., 2009), producing organic material highly enriched in ^{13}C as the sampled glacial sediments show (Fig. 5). The good water solubility of this material (Dubnick et al., 2010) explains the origin of microbial FDOM and $\delta^{13}C$ in DOM. The high nitrogen load is likely due to a release successive to microbial nitrogen fixation in the glacial environment (Telling et al., 2011). DOM under glacial influence is largely characterized by autochthonous signatures.

The elevated values of $SUVA_{254}$ on the other hand indicate the existence of a second source connected to high concentrations of black carbon, derived by organic matter combustion and atmospheric deposition on Tibetan glaciers (Spencer et al., 2014; Wang et al., 2019). Takeuchi (2002) identified cryconite, a powdery mixture of sediment particles, dust and microbes, blown onto the glacier from the surroundings (Hodson et al., 2008), which contribute to dark-coloured organic substances in the cryosphere of Tibet. The high $SUVA_{254}$ can be explained by this. In conclusion, glacial DOM is characterized by both, the autochthonous material derived from the microbiome of the glacier and an allochthonous source, likely cryconite/black carbon type materials that originate from atmospheric deposition. Stream DOM samples in the Qugaqie catchment are largely controlled by endmember DOM signatures from the glacier (Fig. 7d, e). 80% of Qugaqie water discharge originates from glacial meltwater (Adnan et al., 2019) which can explain this large influence, including the low DOC concentrations.

4.2.3. Groundwater springs and intense pastoral activity

The Zhagu catchment shows the lowest mean plant cover and the most pronounced pasture degradation. A groundwater aquifer feeds several first order streams (Tran et al., 2021) and the catchment was arheic during sampling. The collection of groundwater was only possible in Zhagu, due to a lack of open groundwater springs in other catchments. Our data show a relation of high DOC and oxalate concentration with nitrate, phosphate, and potassium at sampling sites of the Zhagu catchment close to springs. The spring endmember further exhibited a high concentration in FDOM (FC 1, FC 3 (microbial-like) and FC 2 (terrestrial-like) - low subset), and had a $\delta^{13}C$ ratio of DOM (mean - 24.2‰) that is richer in ^{13}C compared to those of groundwater samples (mean - 27.2‰) and plants (mean - 26.8‰). Intense pastoral activities have likely led to the high concentration of nutrients and DOC and to the input of organic matter, rich in ^{13}C in spring DOM. This can be interpreted as the result of a strong local influence of yak dung, as was visible around the springs (supplementary materials, Fig. S8, S9). According to Du et al. (2021), yak dung is a relevant source of organic carbon and inorganic nitrogen on the TP. As the $\delta^{13}C$ composition of ungulate faeces fractionates the isotopic signature of the plant fodder source (Ma et al., 2013), this may also in part explain the $\delta^{13}C$ of DOM. In the ordination plots (Fig. 7a, d), terrestrial- and microbial-like FDOM components (FC 3 – high subset, FC 1 and FC 2 – low subset) are connected to spring DOM, indicating that its properties are influenced by yak dung through direct FDOM release and microbial reutilisation. We conclude that Zhagu stream DOM is largely influenced by the groundwater source, affected by degraded pastures and higher nutrient loads through yak dung in the remaining pastures.

4.2.4. Alpine wetlands

Extensive wetlands are scarce in the Nam Co catchment, but still have a large ecological significance in the eastern parts of the TP (Xue et al., 2018). Wetland water samples are chemically distinct from all other sources, as indicated by their large offset to other clusters in the ordination space (Fig. 7b). They have high DOC concentrations, along with $\delta^{13}C$ values resembling those of topsoils (Fig. 5) high oxalate concentrations and high absolute absorbance (A254; Table 2). Shatilla and Carey (2019) reported high DOC concentrations of alpine wetlands of the Alaskan Yukon and high aromaticity, indicating that wetland DOM is primarily plant-derived. In the ordination plots (Fig. 7b) the wetland waters are characterized by strong loading with terrestrial-like FDOM components (FC 1, FC 2, FC 4). Furthermore, wetland water had high magnesium, ammonium, and DIC concentrations and the highest EC of all catchment water samples. The ion enrichment is probably caused by the basin topography of the wetland, which has an accumulation effect from the surroundings. The high ammonium concentrations further indicate high primary production coupled with rapid in-situ degradation and subsequent release of mineral nitrogen. Correspondingly, the microbial, tryptophan-like FDOM component FC 3, suggested to be derived from the activity of the autochthonous microbial community in the water column, is elevated compared to other endmembers.

4.3. Unification of DOM signatures along the stream path

While endmember fingerprints influence DOM signatures in the three catchments, aquatic systems are acknowledged also as mechanistic reactors, exposing DOM to biogeochemical processing during the fluvial pathway (Zark and Dittmar, 2018). In our study unification was exclusively observed in samples of the Qugaqie catchment, where the initial glacial signal with high $SUVA_{254}$ and high ammonium gradually vanishes during the flow path (Fig. 7e). Ammonium is presumably oxidized to nitrate and/or immobilized by riverine microorganisms (Singer et al., 2012), again indicating high volatility of glacial DOM, while alteration of chromophoric DOM is likely due to quick photooxidation (Ni and Li, 2019) or dilution (Jennings et al., 2020). Furthermore, continuous inputs of terrestrial-borne DOM from alpine pastures can explain the downstream change towards more depleted ^{13}C of DOM. Steady inputs hamper unification processes in small catchments (Roebuck et al., 2020) as are reported for larger river systems (Riedel et al., 2016). DOM unification processes exist globally (Kellerman et al., 2018) and processing was identified for several large rivers, like the Yukon river (Shatilla and Carey, 2019), the Ob-Irtysh (Perminova et al., 2019), and the Amazonas (Seidel et al., 2015). We infer, that DOM of large river systems has longer residence times compared to the streams investigated in our study. This substantially decreases the decomposition rate of DOM (Catalán et al., 2016). Concluding, the relatively low stream order, in combination with the diverse source structure and the potential permanent inputs hinder unification processes during the stream path.

4.4. Season specific DOM composition

Seasonality is a major aspect when assessing DOM properties on ecosystem scale (Shatilla and Carey, 2019). Particularly, freshet was found to be a major driver of DOC export in small watersheds, e.g. in permafrost ecosystems (Guggenberger et al., 2008) and in glaciated boreal watersheds of the Arctic (Lafrenière and Sharp, 2004). During freshet, stream samples showed a relatively high load of mineral nitrogen with lower DOC concentrations and more plant-derived DOM compared to other seasons. The results from our study on the TP are exceptional. In fact, the relative

enrichment of plant-derived material was reported during freshet for Siberian rivers (Amon et al., 2012), the Yukon (Shatilla and Carey, 2019) and Arctic watersheds (Lafrenière and Sharp, 2004), but in contrast, this went along with higher DOC concentrations, unlike our findings. During freshet, the high contribution of plant derived DOM is due to mobilization and lateral runoff of DOM in the organic surface soil with snow melt (Guggenberger et al., 2008; Guo and Macdonald, 2006). High mineral nitrogen concentrations are likely a result of a mineralization pulse of lysed microbial cells after thawing (Austnes and Vestgarden, 2008). Our findings indicate that the effect of freshet was smaller than in boreal and tundra biomes. In contrast to these biomes, winter at the Nam Co watershed is characterized by low precipitation and absence of snow cover (Dorji et al., 2013). Consequentially, water discharge from streams is three to four times lower in the non-monsoon season (Yu et al., 2019). Nieberding et al. (2020) found that plant primary production is limited by low water availability. Therefore, physiological reactions of drought resistance in plants (Li et al., 2014; Huang et al., 2021) limit DOM formation. Absence of large freshet effects in the investigated catchments are driven by low water supply, hampering the accumulation of plant-derived DOM.

During the onset of the Indian summer monsoon, DOM was strongly enriched in ^{13}C (up to +7‰) as compared to freshet and baseflow. This was accompanied by a shift in the composition of DOM at unchanged DOC concentrations. In June/July 2018, a coupled decrease of $SUVA_{254}$ and terrestrial-like FDOM components along with less depleted ^{13}C of DOM corresponds to a shift towards a more microbial DOM source during the ISM. As shown for other case studies (Larsen et al., 2010; Zhao et al., 2016), FDOM can track changes in microbial-derived DOM. In our study affected through changing conditions of hydrology and temperature driven by the ISM. Leaching of microbial-derived DOM is especially strong at high soil water contents (Caillon and Schelker, 2020) along with higher soil temperatures (Han et al., 2022b), as is the case during the ISM. Besides, we found a rerouting of draining systems in the investigated catchments. Wadi-like structures with episodic water flow were active in the Niyaqu and Zhagu catchment in June/July 2018. From these channel dead zones, accumulated microbial–derived compounds, such as biofilms can be washed out in great quantities (Wondzell and Ward, 2022). Our data show a pronounced effect of the ISM on DOM composition. During the baseflow in September, $\delta^{13}C$ of DOM decreased compared to the ISM season, concurrently with increased $SUVA_{254}$ and more humic-like FDOM: FC 1, FC 2 and FC 4 (high subset), especially in samples of the Niyaqu catchment. DOM composition after the monsoon influence changed back to a pre-monsoon stage, with DOM inputs mainly derived from soils and plants. Our results suggest unique features of DOM composition and processing with respect to seasonality. Freshet plays a smaller role, compared to boreal and tundra biomes, where this is a more important factor that affects changes in DOM composition. In contrast, the ISM has large effects on DOM composition for these small watersheds of the TP by means of a higher contribution of microbial-derived DOM.

4.5. DOM and biogeochemical signatures in Lake Nam Co

Terminal systems such as oceans or endorheic lakes play an important role in processing DOM. These environments have DOM signatures derived from intense transformation (Goodman et al., 2011; Zark and Dittmar, 2018). Water of Lake Nam Co was characterized by higher concentrations of ions and DIC compared to the water chemistry in catchments (Zhang et al., 2008). We attribute the increased concentration of ions observed in our samples to an evapo-concentration effect (Fujinami and Yasunari, 2001). Zhang et al. (2008) showed that the ion chemistry of Lake Nam Co is relatively unaffected by the ion signatures of inflowing streams, which we substantiate in this study. We show that Nam Co's DOM composition is largely unaffected by seasonality, echoing previous results (Kai et al., 2019). This probably is due to the large water volume and the intense mixing in the dimictic lake. The DOC concentration in the lake was higher compared to the catchment streams, except for sampling sites of Zhagu directly influenced by groundwater. $SUVA_{254}$ and a terrestrial-like FDOM component of the low subset (FC 4) were depleted in lake water samples, while lake water DOM was enriched in ^{13}C with up to +5‰, as compared to stream DOM during freshet and baseflow conditions. Our data are in line with findings from the Rocky Mountains, where DOM of lake and streams was chemically distinct (Goodman et al., 2011). This becomes apparent in the ordination distance between catchments and the lake (Fig. 7d). Microbial-like, tyrosine FDOM (FC 3, low response dataset) was more abundant in lake water samples than in stream DOM and most endmember DOM. This indicates that microbial in-situ production of DOM in the lake is decisive, also indicated by the elevated DOC concentration. Intense photooxidation of the imported chromophoric stream DOM in the lake reduces $SUVA_{254}$, as is visible by 90% lower values compared to stream DOM (Table 1, Table 2). In addition, the enriched ^{13}C of DOM indicates a shift towards autochthonous microbial and algal production. DOM enriched in ^{13}C along with low aromaticity is a typical feature of terminal systems such as large lakes or oceans and are due to microbial and photooxidative processing of riverine DOM as well as autochthonous microbial/algal DOM production (Helms et al., 2014; Spencer et al., 2009).

5. Conclusions

We established a multiparameter dataset of DOM and biogeochemical water signatures (EC, pH, cations and anions, DOC, DIC, $SUVA_{254}$, PARAFAC-resolved FDOM and $\delta^{13}C$ of DOM) for three diverse catchments and for the Lake Nam Co in order to investigate the impact of landscape units on the characteristics and processing of DOM along the course of streams. Stream samples were strongly influenced by terrestrial signatures, having site-specific, unique DOM signatures inherited from glaciers, alpine wetlands, groundwater sources and an operational signature that we attribute to *K. pygmaea* pastures. The high site specificity of DOM, originating from low order streams and endmembers diminishes only slightly with the DOM passage in the streams due to constant terrestrial inputs. However, lake water DOM is almost completely independent of inflowing streams due to photooxidative degradation of primarily phenol-rich, terrestrial-borne organic matter and microbial processing of labile riverine DOM, along with pronounced autochthonous formation of algal- and microbial-derived DOM. The dissolved organic matter composition of Lake Nam Co resembles a quasi-marine terminal environment, while site-specific influences derived from endmembers are largest in the headwaters of streams. We found a loss of site-specific characteristics when comparing lotic regimes with limnic regimes. The mechanisms of DOM processing in the lake should receive more attention in future. Here, investigations implementing lake bathymetry and featuring larger sample sizes are still missing.

Seasonal DOM variations during freshet were found to be less pronounced compared to studies of boreal and tundra biomes. We attribute this to the typical absence of snow cover during winter and therefore the lack of snow-melt driven DOM flush and formation. In contrast, we identified a monsoonal effect on DOC concentrations and DOM signatures, with a pronounced shift towards a strong mobilization of microbial DOM sources. Future studies should consolidate these insights, especially by accounting for the influence of interannual changes of seasonality effects.

Future responses of ecosystems to global change may have pronounced impacts on the concentrations of DOC and inorganic solutes as well as on DOM composition in streams entering Lake Nam Co. A glacier retreat will likely have great effects on the alpine pasture biome in catchments, while the hydrosphere of the Nam Co lake appears relatively uninfluenced by catchment processes. Furthermore, our PCE data indicate a fostered growth of alpine steppe and a greening of the lake shoreline. This may lead to higher DOC concentrations and to a higher proportion of plant-derived, chromophoric DOM exported into the streams and finally to Lake Nam Co. To safeguard lake water quality, grazing control remains crucial. Soil degradation associated with overgrazing and intensive faeces production may lead to a higher input of microbial-derived DOM and of mineral nitrogen to the streams, bearing the risk of eutrophication.

CRediT authorship contribution statement

Philipp Maurischat: Conceptualization, data curation, formal analysis, investigation, validation, visualization, design of experiment, methodology, field work and analyses, writing - original draft, review & editing.

Georg Guggenberger: Design of experiment, writing - review & editing.

Åsmund Rinnan: Additional analysis, methodology, writing - editing.

Karsten Kalbitz: Resources, additional analysis, writing - editing.

Lukas Lehnert: Additional analysis, methodology, writing - editing.

Vinzenz Zerres: Additional analysis, methodology, writing - editing.

Xiaogang Li: Additional analysis, writing – editing.

Tsechoe Dorji: Additional analysis, writing - editing.

Tuong Vi Tran: Additional analysis, writing - editing.

Declaration of competing interest

The authors declare that they have no known competing financial interests or personal relationships that could have appeared to influence the work reported in this paper.

Acknowledgements

The authors owe great gratitude to the ITP-CAS, Lhasa and Beijing branch for their hospitality and help during our sampling campaigns. Further thanks are given to the NAMORS team and for many numerous helpers from the great nations of China. Big thanks to Nicole Börner, Anja Schwarz, Wenggang Kang, Paula Echevarria Galindo, Felix Nieberding, Yuyang Wang, Jinlei Kai, Eike Reinosch and Björn Riedel for helping with sample collection. Thanks to Doreen Fleck for her help with field work and sample treatment. The authors acknowledge the technical support provided by the stackoverflow.com community. Special thanks to Angie Faust for proof reading and to Ina M. Sieber for a thorough review of the manuscript and critical discussion. We would like to thank two anonymous reviewers.

This research is a contribution to the International Research Training Group “Geo-ecosystems in transition on the Tibetan Plateau (TransTiP)”, funded by Deutsche Forschungsgemeinschaft (DFG Grant 317513741/GRK 2309).

Appendix A. Supplementary data

Supplementary data to this article can be found online at https://doi.org/10.1016/j.scitotenv.2022.156542.

References

Adnan, M., Kang, S.-C., Zhang, G.-S., Anjum, M.N., Zaman, M., Zhang, Y.-q., 2019. Evaluation of SWAT model performance on glaciated and non-glaciated subbasins of nam co Lake, southern tibetan plateau, China. J. Mt. Sci. 16 (5).

Amon, R.M.W., Rinehart, A.J., Duan, S., Louchouarn, P., Prokushkin, A., Guggenberger, G., et al., 2012. Dissolved organic matter sources in large Arctic rivers. Geochim. Cosmochim. Acta 94.

Anderson, M.J., Ellingsen, K.E., McArdle, B.H., 2006. Multivariate dispersion as a measure of beta diversity. Ecol. Lett. 9 (6).

Andersson, C.A., Bro, R., 2000. The N-way toolbox for MATLAB. Chemom. Intell. Lab. Syst. 52 (1).

Anesio, A.M., Hodson, A.J., Fritz, A., Psenner, R., Sattler, B., 2009. High microbial activity on glaciers: importance to the global carbon cycle. Glob. Chang. Biol. 15 (4).

Anslan, S., Azizi Rad, M., Buckel, J., Echeverria Galindo, P., Kai, J., Kang, W., et al., 2020. Reviews and syntheses: how do abiotic and biotic processes respond to climatic variations in the nam co catchment (Tibetan Plateau)? Biogeosciences 17 (5).

Austnes, K., Vestgarden, L.S., 2008. Prolonged frost increases release of C and N from a montane heathland soil in southern Norway. Soil Biol. Biochem. 40 (10).

Boix Canadell, M., Escoffier, N., Ulseth, A.J., Lane, S.N., Battin, T.J., 2019. Alpine glacier shrinkage drives shift in dissolved organic carbon export from quasi-chemostasis to transport limitation. Geophys. Res. Lett. 46 (15).

Bolch, T., Yao, T., Kang, S., Buchroithner, M.F., Scherer, D., Maussion, F., et al., 2010. A glacier inventory for the western nyainqentanglha range and the nam co Basin, Tibet, and glacier changes 1976–2009. Cryosphere 4 (3).

Buckel, J., Reinosch, E., Hördt, A., Zhang, F., Riedel, B., Gerke, M., 2020. Insights in a Remote Cryosphere: A Multi Method Approach to Assess Permafrost Occurrence at the Qugaqie Basin, Western Nyainqêntanglha Range, Tibetan Plateau.

Caillon, F., Schelker, J., 2020. Dynamic transfer of soil bacteria and dissolved organic carbon into small streams during hydrological events. Aquat. Sci. 82 (2).

Catalán, N., Marcé, R., Kothawala, D.N., Tranvik, L.J., 2016. Organic carbon decomposition rates controlled by water retention time across inland waters. Nat. Geosci. 9 (7), 501–504.

Chen, L., Gu, W., Li, W., 2019. Why is the east asian summer monsoon extremely strong in 2018?—Collaborative effects of SST and snow cover anomalies. J. Meteorol. Res. 33 (4).

Coch, C., Juhls, B., Lamoureux, S.F., Lafrenière, M.J., Fritz, M., Heim, B., et al., 2019. Comparisons of dissolved organic matter and its optical characteristics in small low and high Arctic catchments. Biogeosciences 16 (23).

Curatola Fernández, G., Obermeier, W., Gerique, A., López Sandoval, M., Lehnert, L., Thies, B., et al., 2015. Land cover change in the Andes of southern Ecuador—Patterns and drivers. Remote Sens. 7 (3).

Damm, B., 1998. Landschaftsdegradation in hochweideregionen tibets als folge natürlicher und anthropogener Einflüsse. Petermanns Geogr. Mitt. 142.

DIN 19266, 2015. pH-Messung- Referenzpufferlösungen zur Kalibrierung von pH-Messeinrichtungen: Deutsches Institut für Normung. 05Beuth Verlag GmbH, Berlin.

DIN EN 27888, 1993. Wasserbeschaffenheit; Bestimmung der elektrischen Leitfähigkeit (ISO 7888:1985); Deutsche Fassung EN 27888:1993: Deutsches Institut für Normung. Beuth Verlag GmbH, Berlin.

Dinno, A., 2017. conover.test: Conover-Iman Test of Multiple Comparisons Using Rank Sums.

Dorji, T., Totland, O., Moe, S.R., Hopping, K.A., Pan, J., Klein, J.A., 2013. Plant functional traits mediate reproductive phenology and success in response to experimental warming and snow addition in Tibet. Glob. Chang. Biol. 19 (2).

Du, Z., Wang, X., Xiang, J., Wu, Y., Zhang, B., Yan, Y., 2021. Yak dung pat fragmentation affects its carbon and nitrogen leaching in Northern Tibet, China. Agric. Ecosyst. Environ. 310 (107301), 1–9. https://doi.org/10.1016/j.agee.2021.107301. https://www.sciencedirect.com/science/article/pii/S0167880921000050.

Dubnick, A., Barker, J., Sharp, M., Wadham, J., Lis, G., Telling, J., et al., 2010. Characterization of dissolved organic matter (DOM) from glacial environments using total fluorescence spectroscopy and parallel factor analysis. Ann. Glaciol. 51 (56).

Faith, D.P., Minchin, P.R., Belbin, L., 1987. Compositional dissimilarity as a robust measure of ecological distance. Vegetatio 69 (1–3).

Federherr, E., Cerli, C., Kirkels, F.M.S.A., Kalbitz, K., Kupka, H.J., Dunsbach, R., et al., 2014. A novel high-temperature combustion based system for stable isotope analysis of dissolved organic carbon in aqueous samples. I: development and validation. Rapid Commun. Mass Spectrom. 28 (23).

Fellman, J.B., Hood, E., Spencer, R.G.M., 2010. Fluorescence spectroscopy opens new windows into dissolved organic matter dynamics in freshwater ecosystems: a review. Limnol. Oceanogr. 55 (6).

Fujinami, H., Yasunari, T., 2001. The seasonal and intraseasonal variability of diurnal cloud activity over the tibetan plateau. JMSJ 79 (6).

Gao, J., 2016. Wetland and its degradation in the yellow river source zone. In: Brierley, G.J. (Ed.), Landscape and Ecosystem Diversity, Dynamics and Management in the Yellow River Source Zone. Springer International Publishing AG, Cham.

Gao, T., Kang, S., Cuo, L., Zhan, T., Zhang, G., Zhang, Y., et al., 2015. Simulation and analysis of glacier runoff and mass balance in the nam co basin, southern tibetan plateau. J. Glaciol. 61 (227).

Gongbuzeren, Huntsinger L., Li, W., 2018. Rebuilding pastoral social-ecological resilience on the Qinghai-tibetan plateau in response to changes in policy, economics, and climate. Ecol. Soc. 23 (2) https://www.jstor.org/stable/26799089.

Goodman, K.J., Baker, M.A., Wurtsbaugh, W.A., 2011. Lakes as buffers of stream dissolved organic matter (DOM) variability: temporal patterns of DOM characteristics in mountain stream-lake systems. J. Geophys. Res. 116 (1), 127.

Görs, S., Rentsch, D., Schiewer, U., Karsten, U., Schumann, R., 2007. Dissolved organic matter along the eutrophication gradient of the Darβ-zingst bodden chain, southern Baltic Sea: I. Chemical characterisation and composition. Mar. Chem. 104 (3–4).

Guggenberger, G., 1994. Acidification effects on dissolved organic matter mobility in spruce forest ecosystems. Environ. Int. 20 (1).

Guggenberger, G., Rodionov, A., Shibistova, O., Grabe, M., Kasansky, O.A., Fuchs, H., et al., 2008. Storage and mobility of black carbon in permafrost soils of the forest tundra ecotone in northern Siberia. Glob. Chang. Biol. 14 (6).

Guo, L., Macdonald, R.W., 2006. Source and transport of terrigenous organic matter in the upper Yukon River: evidence from isotope (δ 13 C, Δ 14 C, and δ 15 N) composition of dissolved, colloidal, and particulate phases. Glob. Biogeochem. Cycles 20 (2).

Han, H., Feng, Y., Chen, J., Xie, Q., Chen, S., Sheng, M., et al., 2022a. Acidification impacts on the molecular composition of dissolved organic matter revealed by FT-ICR MS. Sci. Total Environ. 805.

Han, Y., Qu, C., Hu, X., Wang, P., Wan, D., Cai, P., et al., 2022b. Warming and humidification mediated changes of DOM composition in an alfisol. Sci. Total Environ. 805.

Harris, D., Horwáth, W.R., van Kessel, C., 2001. Acid fumigation of soils to remove carbonates prior to total organic carbon or CARBON-13 isotopic analysis. Soil Sci. Soc. Am. J. 65 (6).

Harris, R.B., 2010. Rangeland degradation on the Qinghai-tibetan plateau: a review of the evidence of its magnitude and causes. J. Arid Environ. 74 (1).

Hedges, J.I., Stern, J.H., 1984. Carbon and nitrogen determinations of carbonate-containing solids. Limnol. Oceanogr. 29 (3).

Helms, J.R., Mao, J., Stubbins, A., Schmidt-Rohr, K., Spencer, R.G.M., Hernes, P.J., et al., 2014. Loss of optical and molecular indicators of terrigenous dissolved organic matter during long-term photobleaching. Aquat. Sci. 76 (3).

Hodson, A., Anesio, A.M., Tranter, M., Fountain, A., Osborn, M., Priscu, J., et al., 2008. Glacial ecosystems. Ecol. Monogr. 78, 1.

Hood, E., Fellman, J., Spencer, R.G.M., Hernes, P.J., Edwards, R., D'Amore, D., 2009. Glaciers as a source of ancient and labile organic matter to the marine environment. Nature 462 (7276).

Hopping, K.A., Knapp, A.K., Dorji, T., Klein, J.A., 2018. Warming and land use change concurrently erode ecosystem services in Tibet. Glob. Chang. Biol. 24 (11).
Hu, E., He, H., Su, Y., Jeppesen, E., Liu, Z., 2016. Use of multi-carbon sources by zooplankton in an oligotrophic Lake in the tibetan plateau. Water 8 (12).
Huang, W., Wang, W., Cao, M., Fu, G., Xia, J., Wang, Z., et al., 2021. Local climate and biodiversity affect the stability of China's grasslands in response to drought. Sci. Total Environ. 768.
Jaffé, R., Yamashita, Y., Maie, N., Cooper, W.T., Dittmar, T., Dodds, W.K., et al., 2012. Dissolved organic matter in headwater streams: compositional variability across climatic regions of North America. Geochim. Cosmochim. Acta 94.
Jennings, E., de Eyto, E., Moore, T., Dillane, M., Ryder, E., Allott, N., et al., 2020. From highs to lows: changes in dissolved organic carbon in a peatland catchment and Lake following extreme flow events. Water 12 (10).
Kai, J., Wang, J., Huang, L., Wang, Y., Ju, J., Zhu, L., 2019. Seasonal variations of dissolved organic carbon and total nitrogen concentrations in nam co and inflowing rivers, Tibet plateau. J. Lake Sci. 31 (4).
Kaiser, K., Miehe, G., Barthelmes, A., Ehrmann, O., Scharf, A., Schult, M., et al., 2008. Turf-bearing topsoils on the central tibetan plateau, China: pedology, botany, geochronology. Catena 73 (3).
Kawahigashi, M., Kaiser, K., Kalbitz, K., Rodionov, A., Guggenberger, G., 2004. Dissolved organic matter in small streams along a gradient from discontinuous to continuous permafrost. Glob. Chang. Biol. 10 (9).
Kellerman, A.M., Guillemette, F., Podgorski, D.C., Aiken, G.R., Butler, K.D., Spencer, R.G.M., 2018. Unifying concepts linking dissolved organic matter composition to persistence in aquatic ecosystems. Environ. Sci. Technol. 52 (5).
Kirkels, F.M.S.A., Cerli, C., Federherr, E., Gao, J., Kalbitz, K., 2014. A novel high-temperature combustion based system for stable isotope analysis of dissolved organic carbon in aqueous samples. II: optimization and assessment of analytical performance. Rapid Commun. Mass Spectrom. 28 (23).
Kothawala, D.N., Ji, X., Laudon, H., Ågren, A.M., Futter, M.N., Köhler, S.J., et al., 2015. The relative influence of land cover, hydrology, and in-stream processing on the composition of dissolved organic matter in boreal streams. J. Geophys. Res. Biogeosci. 120 (8).
Kritzberg, E.S., Hasselquist, E.M., Škerlep, M., Löfgren, S., Olsson, O., Stadmark, J., et al., 2020. Browning of freshwaters: consequences to ecosystem services, underlying drivers, and potential mitigation measures. AMBIO J. Hum. Environ. 49 (2).
Lafrenière, M.J., Sharp, M.J., 2004. The concentration and fluorescence of dissolved organic carbon (DOC) in glacial and nonglacial catchments: interpreting hydrological flow routing and DOC sources. Arct. Antarct. Alp. Res. 36 (2).
Larsen, L.G., Aiken, G.R., Harvey, J.W., Noe, G.B., Crimaldi, J.P., 2010. Using fluorescence spectroscopy to trace seasonal DOM dynamics, disturbance effects, and hydrologic transport in the Florida Everglades. J. Geophys. Res. 115 (G3).
Lau, M.P., 2021. Linking the dissolved and particulate domain of organic carbon in inland waters. J. Geophys. Res. Biogeosci. 126 (5), 1–4.
Lehnert, L.W., Meyer, H., Wang, Y., Miehe, G., Thies, B., Reudenbach, C., et al., 2015. Retrieval of grassland plant coverage on the tibetan plateau based on a multi-scale, multi-sensor and multi-method approach. Remote Sens. Environ. 164. https://www.sciencedirect.com/science/article/pii/S0034425715001625.
Lehnert, L.W., Miehe, G., Heitkamp, F., Seeber, E., Manson-Jones, K., Schleuss, P.-M., 2015. Mechanisms and Consequences of Tibetan Grassland Degradation From Soil Profile to Ecosystem Scale.
Lehnert, L.W., Wesche, K., Trachte, K., Reudenbach, C., Bendix, J., 2016. Climate variability rather than overstocking causes recent large scale cover changes of tibetan pastures. Sci. Rep. 6 (24367), 1–8.
Leinemann, T., Preusser, S., Mikutta, R., Kalbitz, K., Cerli, C., Höschen, C., et al., 2018. Multiple exchange processes on mineral surfaces control the transport of dissolved organic matter through soil profiles. Soil Biol. Biochem. 118 (1).
Li, X., Yang, Y., Ma, L., Sun, X., Yang, S., Kong, X., et al., 2014. Comparative proteomics analyses of Kobresia pygmaea adaptation to environment along an elevational gradient on the central tibetan plateau. PLOS ONE 9 (6).
Li, Y., Xiao, K., Du, J., Han, B., Liu, Q., Niu, H., 2021. Spectroscopic fingerprints to track the fate of aquatic organic matter along an alpine headstream on the Tibetan Plateau. Sci. Total Environ. 792 (148376), 1–9.
Liu, S., Zamanian, K., Schleuss, P.-M., Zarebanadkouki, M., Kuzyakov, Y., 2018. Degradation of tibetan grasslands: consequences for carbon and nutrient cycles. Agric. Ecosyst. Environ. 252.
Ma, X., Ambus, P., Wang, S., Wang, Y., Wang, C., 2013. Priming of soil carbon decomposition in two Inner Mongolia grassland soils following sheep dung addition: a study using 13C natural abundance approach. PLOS ONE 8 (11).
Massicotte, P., Frenette, J.-J., 2013. A mechanistic-based framework to understand how dissolved organic carbon is processed in a large fluvial lake. Limnol. Oceanogr. 3 (1).
Miehe, G., Miehe, S., Kaiser, K., Jianquan, L., Zhao, X., 2008. Status and dynamics of the Kobresia pygmaea ecosystem on the Tibetan Plateau. AMBIO J. Hum. Environ. 37 (4).
Miehe, G., Schleuss, P.-M., Seeber, E., Babel, W., Biermann, T., Braendle, M., 2019. The Kobresia pygmaea ecosystem of the Tibetan highlands - Origin, functioning and degradation of the world's largest pastoral alpine ecosystem: Kobresia pastures of Tibet. Sci. Total Environ. 648.
Mosher, J.J., Kaplan, L.A., Podgorski, D.C., McKenna, A.M., Marshall, A.G., 2015. Longitudinal shifts in dissolved organic matter chemogeography and chemodiversity within headwater streams: a river continuum reprise. Biogeochemistry 124 (1–3).
Murphy, K.R., Stedmon, C.A., Wenig, P., Bro, R., 2014. OpenFluor– an online spectral library of auto-fluorescence by organic compounds in the environment. Anal. Methods 6 (3).
Ni, M., Li, S., 2019. Biodegradability of riverine dissolved organic carbon in a Dry-Hot Valley region: initial trophic controls and variations in chemical composition. J. Hydrol. 574.
Nieberding, F., Wille, C., Fratini, G., Asmussen, M.O., Wang, Y., Ma, Y., 2020. A long-term (2005–2019) eddy covariance data set of CO2;/H2O fluxes from the Tibetan alpine steppe. Earth Syst. Sci. Data 12 (4).
Nieberding, F., Wille, C., Ma, Y., Wang, Y., Maurischat, P., Lehnert, L., 2021. Winter daytime warming and shift in summer monsoon increase plant cover and net CO 2 uptake in a central Tibetan alpine steppe ecosystem. J. Geophys. Res. Biogeosci. 126, 1–20.
Oksanen, J., Blanchet, F.G., Friendly, M., Kindt, R., Legendre, P., McGlinn, D., 2020. vegan: Community Ecology Package.
Perminova, I.V., Shirshin, E.A., Zherebker, A., Pipko, I.I., Pugach, S.P., Dudarev, O.V., et al., 2019. Signatures of molecular unification and progressive oxidation unfold in dissolved organic matter of the Ob-Irtysh River system along its path to the Arctic Ocean. Sci. Rep. 9 (1).
Qiu, J., 2008. China: The third pole. Nat. News 454 (7203). https://www.nature.com/news/2008/080723/full/454393a.html.
Qiu, J., 2016. Trouble in Tibet. Nat. News 529 (7585). https://www.nature.com/news/trouble-in-tibet-1.19139.
R Core Team, 2013. R: A Language and Environment for Statistical Computing. R Foundation for Statistical Computing, Vienna, Austria.
Riano, D., Chuvieco, E., Salas, J., Aguado, I., 2003. Assessment of different topographic corrections in landsat-TM data for mapping vegetation types (2003). IEEE Trans. Geosci. Remote Sensing 41 (5).
Riedel, T., Zark, M., Vähätalo, A.V., Niggemann, J., Spencer, R.G.M., Hernes, P.J., et al., 2016. Molecular signatures of biogeochemical transformations in dissolved organic matter from ten world Rivers. Front. Earth Sci. 4 (85), 1–16.
Roebuck, J.A., Seidel, M., Dittmar, T., Jaffé, R., 2020. Controls of land use and the river continuum concept on dissolved organic matter composition in an anthropogenically disturbed subtropical watershed. Environ. Sci. Technol. 54 (1).
Roulet, N., Moore, T.R., 2006. Environmental chemistry: browning the waters. Nature 444, 7117.
Roy, D.P., Kovalskyy, V., Zhang, H.K., Vermote, E.F., Yan, L., Kumar, S.S., 2016. Characterization of Landsat-7 to Landsat-8 reflective wavelength and normalized difference vegetation index continuity. Remote Sens. Environ. 185 (1).
Schleuss, P.M., Heitkamp, F., Seeber, E., Spielvogel, S., Miehe, G., Guggenberger, G., Kuzyakov, Y., 2015. Mechanisms of soil degradation and its consequences for soil organic carbon storage on alpine grasslands of the Tibetan Plateau. Int. Symp. Soil Org. Matter 5, 1–19.
Seidel, M., Yager, P.L., Ward, N.D., Carpenter, E.J., Gomes, H.R., Krusche, A.V., et al., 2015. Molecular-level changes of dissolved organic matter along the Amazon River-to-ocean continuum. Mar. Chem. 177.
Shatilla, N.J., Carey, S.K., 2019. Assessing inter-annual and seasonal patterns of DOC and DOM quality across a complex alpine watershed underlain by discontinuous permafrost in Yukon, Canada. Hydrol. Earth Syst. Sci. 23 (9).
Singer, G.A., Fasching, C., Wilhelm, L., Niggemann, J., Steier, P., Dittmar, T., et al., 2012. Biogeochemically diverse organic matter in alpine glaciers and its downstream fate. Nat. Geosci. 5 (10).
Singh, S., Dash, P., Silwal, S., et al., 2017. Influence of land use and land cover on the spatial variability of dissolved organic matter in multiple aquatic environments. Environ. Sci. Pollut. Res. 24, 14124–14141. https://doi.org/10.1007/s11356-017-8917-5.
Song, C., Huang, B., Richards, K., Ke, L., Hien Phan, V., 2014. Accelerated lake expansion on the Tibetan Plateau in the 2000s: induced by glacial melting or other processes? Water Resour. Res. 50 (4).
Song, C., Wang, G., Haghipour, N., Raymond, P.A., 2020. Warming and monsoonal climate lead to large export of millennial-aged carbon from permafrost catchments of the Qinghai-Tibet plateau. Environ. Res. Lett. 15 (7). https://iopscience.iop.org/article/10.1088/1748-9326/ab83ac.
Speetjens, N., Tanski, G., Martin, V., Wagner, J., Richter, A., Hugelius, G., 2020. Landscape-driven Carbon Export From Small Coastal Permafrost Watersheds.
Spencer, R.G.M., Stubbins, A., Hernes, P.J., Baker, A., Mopper, K., Aufdenkampe, A.K., et al., 2009. Photochemical degradation of dissolved organic matter and dissolved lignin phenols from the Congo River. J. Geophys. Res. 114 (G3).
Spencer, R.G.M., Guo, W., Raymond, P.A., Dittmar, T., Hood, E., Fellman, J., et al., 2014. Source and biolability of ancient dissolved organic matter in glacier and lake ecosystems on the tibetan plateau. Geochim. Cosmochim. Acta 142.
Takeuchi, N., 2002. Optical characteristics of cryoconite (surface dust) on glaciers: the relationship between light absorbency and the property of organic matter contained in the cryoconite. Ann. Glaciol. 34.
Telling, J., Anesio, A.M., Tranter, M., Irvine-Fynn, T., Hodson, A., Butler, C., et al., 2011. Nitrogen fixation on Arctic glaciers, Svalbard. J. Geophys. Res. 116 (G3).
Tibetan pastoralists, 2019. Information on local ecological knowledge and yak stocking numbers as well as transhumance strategies. Orally Nam Co catchment.
Tran, T.V., Buckel, J., Maurischat, P., Tang, H., Yu, Z., Hördt, A., et al., 2021. Delineation of a quaternary aquifer using integrated hydrogeological and geophysical estimation of hydraulic conductivity on the Tibetan Plateau, China. Water 13 (10).
VDLUFA, 2012. Kongressband 2012 Passau: Vorträge zum Generalthema: Nachhaltigkeitsindikatoren für die Landwirtschaft: Bestimmung und Eignung. VDLUFA-Verl, Darmstadt.
Vermote, E.F., Tanre, D., Deuze, J.L., Herman, M., Morcette, J.J., 1997. Second simulation of the satellite signal in the solar Spectrum, 6S: an overview. IEEE Trans. Geosci. Remote Sens. 35 (3).
Wang, J., Zhu, L., Daut, G., Ju, J., Lin, X., Wang, Y., et al., 2009. Investigation of bathymetry and water quality of Lake Nam Co, the largest lake on the central Tibetan Plateau, China. Limnology 10 (2).
Wang, J., Zhu, L., Wang, Y., Ju, J., Xie, M., Daut, G., 2010. Comparisons between the chemical compositions of lake water, inflowing river water, and lake sediment in nam co, central tibetan plateau, China and their controlling mechanisms. J. Great Lakes Res. 36 (4).
Wang, J., Huang, L., Ju, J., Daut, G., Ma, Q., Zhu, L., et al., 2020. Seasonal stratification of a deep, high-altitude, dimictic lake: nam co, tibetan plateau. J. Hydrol. 584 (7).
Wang, Y., Hu, M., Lin, P., Tan, T., Li, M., Xu, N., et al., 2019. Enhancement in particulate organic nitrogen and light absorption of humic-like substances over tibetan plateau due to long-range transported biomass burning emissions. Environ. Sci. Technol. 53 (24).

Weishaar, J.L., Aiken, G.R., Bergamaschi, B.A., Fram, M.S., Fujii, R., Mopper, K., 2003. Evaluation of specific ultraviolet absorbance as an indicator of the chemical composition and reactivity of dissolved organic carbon. Environ. Sci. Technol. 37 (20).

Wickham, H., Averick, M., Bryan, J., Chang, W., François, R., McGowan, L., 2019. Welcome to the Tidyverse. JOSS 4 (43).

Wondzell, S.M., Ward, A.S., 2022. The channel source hypothesis: empirical evidence for in-channel sourcing of dissolved organic carbon to explain hysteresis in a headwater mountain stream. Hydrol. Process. 36 (5), 1–12.

Wymore, A.S., Rodríguez-Cardona, B., McDowell, W.H., 2016. Understanding dissolved organic matter biogeochemistry through in situ nutrient manipulations in stream ecosystems. J. Vis. Exp. 116.

Xu, Z., Wan, S., Colin, C., Clift, P.D., Chang, F., Li, T., 2021. Enhancements of Himalayan and Tibetan erosion and the produced organic carbon burial in distal tropical marginal seas during the Quaternary glacial periods: an integration of sedimentary records. J. Geophys. Res. Earth Surf. 126 (3), 1–17.

Xue, Z., Lyu, X., Chen, Z., Zhang, Z., Jiang, M., Zhang, K., et al., 2018. Spatial and temporal changes of wetlands on the Qinghai-tibetan plateau from the 1970s to 2010s. Chin. Geogr. Sci. 28 (6).

Yamashita, Y., Scinto, L.J., Maie, N., Jaffé, R., 2010. Dissolved organic matter characteristics across a subtropical Wetland's landscape: application of optical properties in the assessment of environmental dynamics. Ecosystems 13 (7).

Yao, T., Thompson, L.G., Mosbrugger, V., Zhang, F., Ma, Y., Luo, T., et al., 2012. Third pole environment (TPE). Environ. Dev. 3.

Yu, Z., Wu, G., Keys, L., Li, F., Yan, N., Qu, D., et al., 2019. Seasonal variation of chemical weathering and its controlling factors in two alpine catchments, nam co basin, central tibetan plateau. J. Hydrol. 576.

Yu, Z., Wu, G., Li, F., Chen, M., Vi Tran, T., Liu, X., 2021. Glaciation enhanced chemical weathering in a cold glacial catchment, western Nyaingêntanglha Mountains, central Tibetan Plateau. J. Hydrol. 597 (5).

Zark, M., Dittmar, T., 2018. Universal molecular structures in natural dissolved organic matter. Nat. Commun. 9 (1). https://www.nature.com/articles/s41467-018-05665-9.

Zhang, H., Ding, M., Li, L., Liu, L., 2019. Continuous Wetting on the Tibetan Plateau during 1970–2017. Water 11 (12).

Zhang, Q., Kang, S., Wang, F., Li, C., Xu, Y., 2008. Major ion geochemistry of Nam Co lake and its sources, Tibetan Plateau. Aquat. Geochem. 14 (4).

Zhang, W., Zhou, T., Zhang, L., 2017. Wetting and greening tibetan plateau in early summer in recent decades. J. Geophys. Res. Atmos. 122 (11).

Zhang, Z., Qin, J., Sun, H., Yang, J., Liu, Y., 2020. Spatiotemporal dynamics of dissolved organic carbon and freshwater Browning in the zoige alpine wetland, northeastern Qinghai-tibetan plateau. Water 12 (9).

Zhao, Y., Song, K., Wen, Z., Li, L., Zang, S., Shao, T., et al., 2016. Seasonal characterization of CDOM for lakes in semiarid regions of Northeast China using excitation–emission matrix fluorescence and parallel factor analysis (EEM–PARAFAC). Biogeosciences 13 (5).

Zhao, Z., Gonsior, M., Schmitt-Kopplin, P., et al., 2019. Microbial transformation of virus-induced dissolved organic matter from picocyanobacteria: coupling of bacterial diversity and DOM chemodiversity. ISME J. 13, 2551–2565. https://doi.org/10.1038/s41396-019-0449-1.

Zhong, L., Ma, Y., Xue, Y., Piao, S., 2019. Climate change trends and impacts on vegetation greening over the tibetan plateau. J. Geophys. Res. Atmos. 124 (14).

Zhou, Y., Zhou, L., He, X., Jang, K.-S., Yao, X., Hu, Y., et al., 2019. Variability in dissolved organic matter composition and biolability across gradients of glacial coverage and distance from glacial terminus on the Tibetan plateau. Environ. Sci. Technol. 53 (21).